MICROWAVE-ASSISTED LIGNIN DEPOLYMERIZATION FOR BIO-OIL AND PHENOIC MONOMER PRODUCTION

by

Ningning Zhou

Submitted in partial fulfilment of the requirements
for the degree of Master of Science

at

Dalhousie University
Halifax, Nova Scotia
November 2020

Table of Contents

List of Tables

List of Figures

Abstract

The population expansion, industrial development and environmental deterioration drive a shift from petroleum-refinery to biorefinery. Lignin, is an abundantly available bioresource that can be valorized to produce a wide array of bio-based products. However, depolymerization of this macropolymer is costly and technically difficult.

This research evaluated a microwave-assisted depolymerization of lignin in the presence of formic acid to produce bio-oil and phenolic monomers. The amount of formic acid was identified as the most critical factor influencing product yields. Depolymerization conditions for alkaline and de-alkaline were optimized. An "in-house" downstream processing protocol was developed, and demonstrated efficient to recover high-quality bio-oil. Acidic condition favored the product recovery than neutral or basic conditions. In terms of reaction medium, ethanol was better than water. This work provided a feasible route to depolymerize lignin under mild condition (temperature of 230°C) using renewable reagents (formic acid and ethanol) and energy-efficient heating source (microwave irradiation).

List of Abbreviations Used

HTL	hydrothermal liquefaction
MW	microwave
BO	bio-oil
PM	phenolic monomer
SR	solid residue
DAF	dry ash free
CCD	central composite design
RSM	response surface methodology
LCCs	lignin-carbohydrate complexes
LS	lignosulfonate
KL	kraft lignin
SL	soda lignin
OSL	organosolv lignin
BL	bio-lignin
EL	eucalyptus lignin
HL	hardwood lignin
FA	formic acid
THF	tetrahydrofuran
EG	ethylene glycol
DMSO	dimethyl sulfoxide
DMF	dimethyl formamide
MSTFA	N-Methyl-N-(trimethylsilyl)-trifluoroacetamide
ICP	inductively Coupled Plasma
GCMS	gas chromatograph-mass spectrometry
TIC	total ion chromatography
GPC	gel permeation chromatography
HPLC	high-performance liquid chromatography
NMR	nuclear magnetic resonance
ANOVA	analysis of variance
NPP	normal probability plot
LSD	least significant difference
Mn	number average molecular mass
Mw	weight average molecular mass
PDI	polydispersity index
LLE	liquid-liquid extraction
H type	p-hydroxyphenyl/phenol type
G type	guaiacyl/guaiacol type
S type	syringyl/syringol type
ICFAR	Institute for Chemical and Fuels from Alternative Resources

Acknowledgements

I would like to express my sincere gratitude to my supervisor Dr. Quan (Sophia) He, for her continuous support, patient guidance and strong encouragement throughout my MSc study. I have been extremely lucky to have a supervisor who cared so much about my work and responded to my queries so promptly. It was my honor to share of her exceptional scientific knowledge and nice human qualities.

I am also very grateful to my co-supervisor Dr. Chunbao (Charles) Xu, for his constructive suggestions and technical guidance throughout this research. My sincere gratitude extends to my supervisory committee members, Dr. Vasantha Rupasinghe and Dr. Haibo Niu, for their support and valuable advices. Their contributions to this research are greatly appreciated.

I also have to say a special word of thanks to Dr. Jie Yang for his mentoring and encouragement. Last but not least, I would like to thank my families and friends for their unconditional support, encouragement and love, and without which I would not have come this far.

Chapter 1: Introduction

1.1. Background

Petroleum is well known to serve as the lifeblood of chemical industry in the past century. It is the raw material for basic chemicals and is used to produce a tremendous wealth of products. However, the contexts of population expansion, environmental deterioration, resource depletion and industrial development suggest that the chemical industry should be increasingly focusing on renewable resources. To achieve the sustainable development goals set by the United Nations, one strategy is to reduce the dependency on petroleum refinery by shifting to biorefinery, which refers to the idea of maximizing the value of biomass by integrating biomass conversion processes and advanced equipment to produce biofuels, biomaterials, and value-added chemicals (Li & Takkellapati, 2018; Yuan et al., 2013).

As the main non-food component of biomass, lignocellulose forms the foundation of biorefinery industry. Lignocellulose is composed of three main polymeric fractions including lignin, cellulose and hemicellulose. Second to cellulose, lignin is the most abundant natural biopolymer on earth, accounting for 20-35% of the weight of lignocellulosic biomass, and it is the largest warehouse of renewable aromatic chemicals (Feofilova & Mysyakina, 2016; Li & Takkellapati, 2018).

Lignin offers significant opportunities for enhanced operation of the lignocellulosic biorefinery industry due to its extreme abundance, wide availability, rich variety of attached functional groups, biodegradability, biocompatibility, reinforcing capability, hydrophilic and lipophilic structures, antioxidant property, as well as other potential pharmacological activities (Xu & Ferdosian, 2017). The current and potential applications of lignin can be divided into three categories, including (1) heat, power, syngas and green fuel products; (2) macromolecules (e.g. binders and carbon fibers); and (3) low molecular weight aromatic/phenolic compounds (e.g. phenol and vanillin) (Holladay et al., 2007).

Although lignin holds great potential as a renewable source of biofuels, biomaterials and aromatic chemicals, it is substantially underutilized in biorefinery industry at present as compared to the polysaccharides (cellulose and hemicellulose) and was traditionally used for low-tech heat and power generation as a by-product from pulping industry and cellulosic ethanol production (Li & Takkellapati, 2018; Pilar Vinardell & Mitjans, 2017; Shao et al., 2018). The structural complexity, inherent heterogeneity and recalcitrance of lignin severely restrict its high-value

applications. To date, almost all the current commercial uses of lignin only take the advantage of its polymer and polyelectrolyte properties to produce macromolecules with relatively low value and limited applications such as binders, dispersants, emulsifiers and sequestrants (Holladay et al., 2007). In order to satisfy the enormous and diverse demand for aromatic chemicals, obtaining small aromatic building blocks of great value efficiently through lignin depolymerization is regarded as a challenging but viable long-term opportunity.

1.2. Lignin Depolymerization

A wide variety of depolymerization technologies have been studied with the aim to convert lignin into value-added chemicals. These methods can be summarized into three main categories, including biological, chemical and thermal techniques. In most cases, chemical depolymerization of lignin is carried out in a combination with thermal techniques, known as thermochemical depolymerization. Biological depolymerization, which takes the advantage of lignin-degrading enzymes, is less favorable due to its poor productivity and low yield as compared to thermochemical lignin depolymerization (Chen & Wan, 2017). Thermochemical depolymerization technologies can be further divided into several sub-categories such as pyrolysis, hydrothermal liquefaction (HTL), reductive depolymerization/hydrogenolysis, oxidative depolymerization, as well as homogenous acid/base catalyzed depolymerization (Xu et al., 2014).

Most of the thermal and chemical depolymerization technologies have long been carried out using conventional electric resistance heating. In light of a growing awareness of "use of renewable feedstocks", and "design for energy efficiency" as two of the twelve key principles of green chemistry (Warner, 2012), microwave (MW) irradiation has stood out as an attractive new heating source due to its fast heating rate, lower energy consumption and high heating efficiency. To our knowledge, MW irradiation has been investigated in many studies as a heating source for lignocellulosic biomass pretreatment such as delignification and cellulose solubilization. For converting biomass into value-added products, most of the studies have been focused on MW-assisted pyrolysis for bio-oil (BO) production under harsh conditions. However, studies on MW-assisted solvolysis of lignocellulosic biomass under mild conditions are relatively limited in the literature. In any case, the design of an energy efficient and stable system capable of working under mild reaction conditions provides a significant step forward in lignin depolymerization technologies. Based on these premises, our research interest lies in MW-assisted lignin depolymerization under mild conditions.

Besides the challenge related to energy intensity, another challenge associated with lignin depolymerization is that most lignin-derived products are highly oxygenated species with low energy potential. In order to make lignin-derived products competitive with fuels and chemicals obtained from traditional petroleum refinery, a wide variety of noble metal-based catalysts have been employed for lignin depolymerization processes, such as ruthenium (Ru), rhodium (Rh), palladium (Pd), and platinum (Pt) (Hu et al., 2019; Y. Huang et al., 2017; Onwudili, 2015; Oregui Bengoechea et al., 2015). However, the continuous need for noble metals of low abundance not only arouses economic concerns but also poses threats to the environment due to extensive mining and refinement of metal ores. Moreover, it is estimated that less than 1% of the spent metal-based catalysts are recycled, resulting in the lower economic viability of heterogeneous catalytic lignin depolymerization (Ludwig & Schindler, 2017).

To address some of these challenges, this work investigated the feasibility of lignin depolymerization under energy-efficient microwave irradiation without using any noble metal-based catalysts. The target bioproducts were bio-oil (BO) and phenolic monomers (PM). Formic acid (FA), a biomass-derived simple carboxylic acid was used as an *in situ* hydrogen donor for reductive depolymerization/hydrogenolysis of lignin. As one of the main side-products obtaining from cellulose and hemicellulose hydrolysis, the use of FA for MW-assisted thermochemical lignin conversion into value-added products perfectly meets the sustainability and green process criteria (Chen et al., 2020). The proposed approach was therefore, extremely attractive from an economic, environmental and process intensification perspective.

1.3. Research Objectives and Hypotheses

The overall objective of the research is to evaluate the feasibility of MW-assisted lignin depolymerization in the presence of FA for BO and PM production. The specific objectives include:

1. To investigate the effects of critical process variables on the yield of BO and PM derived from MW-assisted lignin depolymerization.
2. To optimize the lignin depolymerization conditions for maximizing the yield of the targeted products BO and PM.
3. To explore the effects of downstream processing method on products generated from MW-assisted lignin depolymerization.
4. To carry out MW-assisted lignin depolymerization in the aqueous solvent system and compare it to lignin depolymerization in ethanolic solvent system.

The research hypothesis is that MW-assisted lignin depolymerization under mild conditions with the assistance of FA could be an efficient route to produce BO and PM. It was also hypothesized that the process variables associated with reaction conditions (e.g. temperature and FA loading), the type of lignin feedstock and the selection of reaction solvent might create large variability in the yield and physicochemical properties of lignin-derived product.

1.4. Thesis Organization

Chapter 2 presents a literature review of the contents relevant to this research, including lignin as a renewable feedstock, the methods for lignin depolymerization, fundamentals of microwave irradiation and its application in lignin depolymerization. Chapter 3 provides a description of the materials and methods used in this study, including the setup procedures of MW-assisted lignin depolymerization, separation of reaction products, as well as the methods of feedstock and product characterization. Chapter 4 aims to get a preliminary understanding about the effects of critical process variables on the lignin-derived product yield by using a response surface methodology (RSM). In continuation to the previous chapter, Chapter 5 presents the development of regression models for product yields and the optimization of MW-assisted lignin depolymerization for bio-oil (BO) and phenolic monomers (PM) production. Chapter 6 depicts the development of an "in-house" downstream processing protocol as well as the investigation of the impacts of downstream processing method on products derived from MW-assisted lignin depolymerization. In Chapter 4, 5 and 6, MW-assisted lignin depolymerization was conducted in an ethanolic solvent system. Chapter 7 explores MW-assisted lignin depolymerization in an aqueous solvent system, and a comparison of the solvent effect on product yield between ethanol and water was presented as well. Chapter 8 provides the overall conclusions of this study and gives recommendations for the future work.

Chapter 2: Review of Literature

2.1. Lignin: A Renewable Feedstock

2.1.1. Structural Characteristics of Lignin

Lignin contributes to the strength and rigidity of plant cell wall by filling the space between cellulose and hemicellulose, as well as acting like a resin to bind lignocellulose matrix together (Liu et al., 2015). Moreover, lignin exhibits several distinct properties such as antioxidant activity, antimicrobial activity, and ultraviolet absorption (Cheng et al., 2018). The molecular weight, chemical composition and amount of lignin vary substantially with botanical species, and even with plant individuals and morphological parts of a plant. The lignin content in biomass is descending in the order of softwood > hardwoods > grasses (Zakzeski et al., 2010).

In terms of structural characteristics, lignin is a highly-branched three-dimensional heterogeneous biopolymer formed by radical polymerization of three primary monolignols as shown in Fig. 2.1, including p-coumaryl, coniferyl and sinapyl alcohols that contain zero, one, and two methoxyl groups respectively (Chen & Wan, 2017). Correspondingly, these monolignol precursors are biosynthesized and incorporated into lignin macromolecules in the form of three phenylpropanoid units, namely p-hydroxyphenyl (H), guaiacyl (G) and syringyl (S) units (Feofilova & Mysyakina, 2016; Xu et al., 2014). As presented in Fig. 2.2, radical coupling of these monolignols results in the formation of different inner-unit linkages, which are mainly ether bonds (e.g. β-O-4, α-O-4 and 4-O-5) and C-C bonds (e.g. β-1, β-5, 5-5' and β-β) (Wang et al., 2016). Different types of linkages between two lignin monolignols are classified by using Greek alphabets (e.g. α, β and γ) and Arabic numerals (from 1 to 6) to label carbon atoms in aliphatic side chains and aromatic rings (Cheng et al., 2018). Over two-thirds of the inner-unit linkages are ether bonds, especially β-O-4-aryl bond, which makes up approximately 46% and 60% of linkages in softwood and hardwood respectively (Azadi et al., 2013). Various functional groups on lignin structure with major contribution to its reactivity in chemical reactions involve methoxyl, aliphatic hydroxyl, phenolic hydroxyl, benzyl alcohol, noncyclic benzyl ether and carbonyl groups (Pandey & Kim, 2011).

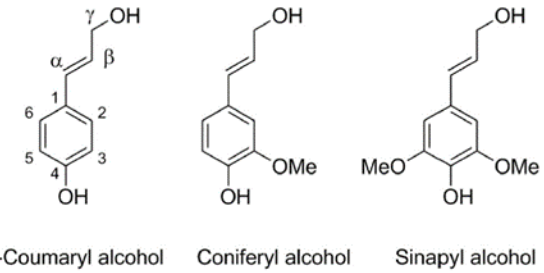

Figure 2.1 Three primary monolignols as lignin building block. Adapted from (Chen & Wan, 2017)

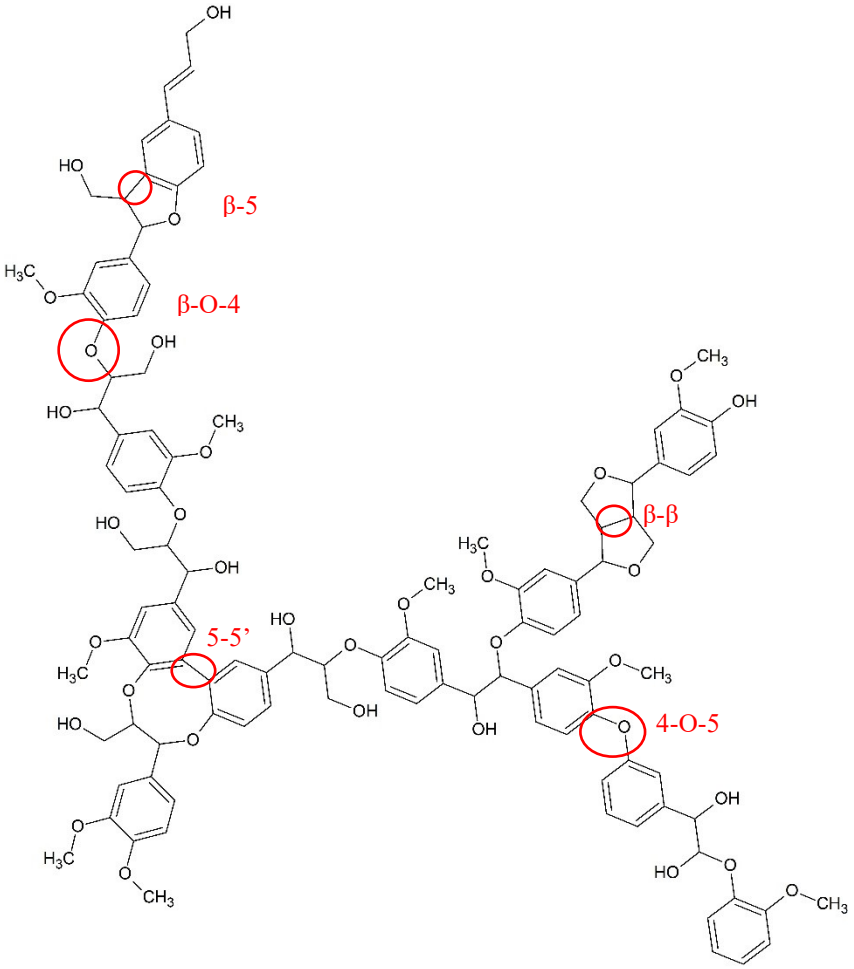

Figure 2.2 Representative lignin substructure

2.1.2. Sources of Technical Lignin

Effective separation of lignin with high yield, high purity and less condensed structure is critically important in the lignocellulose biorefinery process. Isolation of different components of lignocellulosic biomass, also known as lignocellulose fractionation, is a major challenge due to the structural complexity of plant cell walls and high crystallinity of cellulose (Cheng et al., 2018).

It is also believed that certain reactive components called lignin-carbohydrate complexes (LCCs), which are linked to hemicellulose by covalent bonds, severely restrict the separation of lignin in pulping and paper industry (Wang et al., 2019; You et al., 2015). Many chemical processes have been developed throughout the years to isolate lignin from lignocellulosic biomass at both industrial and analytical scales (Duval & Lawoko, 2014). As the result of chemical and physical treatments during lignocellulose fractionation (or lignin isolation), native lignin undergoes structural changes of different degrees and the obtained technical lignins (or isolated lignins) are unique in terms of their chemical structure, molecular weight, biological activity, impurity profile, and polydispersity (Li & Takkellapati, 2018). Therefore, technical lignins are usually classified in accordance with the industrial separation processes they are from (e.g. the sulfite, kraft, soda and organosolv processes).

Four types of technical lignin that have been commercialized and extensively investigated include lignosulfonate (LS), kraft lignin (KL), soda lignin (SL) and organosolv lignin (OSL), whose annual outputs are summarized in a descending order as shown in Table 2.1 (Li & Takkellapati, 2018). The kraft process is the most dominant pulping process in which a mixture of sodium hydroxide (NaOH) and sodium sulfide (Na_2S), known as white liquor, is used to digest lignocellulose at high temperatures (423-453K) (Zakzeski et al., 2010). Cellulose is separated by filtration while lignin and hemicellulose are solubilized into a liquid phase called black liquor (Li & Takkellapati, 2018). LignoBoost technology, a patent owned by Metso Corporation that takes the advantage of a series of processes including acid precipitation, dewatering, redissolution and filtration, was developed in 2013 by a group of Swedish inventors to effectively separate lignin from black liquor and produce KL with rich phenolic hydroxyl groups (Strassberger et al., 2014). Since KL contains a small amount of sulfur due to the use of Na_2S, it could be less suitable for chemical functionalization, especially when catalysis is required (Agarwal et al., 2018; Duval & Lawoko, 2014). Although kraft process is regarded as industrially advantageous with considerable infrastructures established worldwide, it is not likely to serve as the primary source of lignin for the biorefinery industry since lignin is consumed as fuel for process heating (Zakzeski et al., 2010). The sulfite process yielding LS is also common in the pulp and paper industry and is by far the largest producer of lignin, in which a large number of sulfonate groups are incorporated into lignin structure on arenes by using aqueous solution of sulfites (e.g. Na_2SO_3, $MgSO_3$, $CaSO_3$, and $(NH_4)_2SO_3$) at different pH (between 1-13.5) (Li & Takkellapati, 2018). In other words, the sulfite

process can be carried out in either alkaline, neutral, or acidic conditions, which depends on the selection of (bi)sulfite salts (Schutyser et al., 2018). LS is typically water-soluble and exhibits a relatively higher average molecular weight as well as surfactant properties, making it a promising candidate in several industries as dispersant, water reducer in concrete or viscosity reducer (Duval & Lawoko, 2014; Zakzeski et al., 2010). At conditions similar to kraft process, soda process uses NaOH to dissolve lignin from lignocellulosic biomass, with the major difference that there is no implementation of Na_2S. SL is therefore sulfur free and particularly attractive for polymer applications (Schutyser et al., 2018). Organosolv pulping is a process wherein lignocellulosic biomass is treated with an organic solvent (e.g. alcohols, polyols, organic acids and ketones), sometimes in combination with mineral acids and/or water (Lancefield et al., 2017). This process enables efficient separation of lignocellulosic components including a solid cellulose pulp, a lignin precipitate and an aqueous hemicellulose-derived stream, yielding high purity OSL with very low sulfur content (Schutyser et al., 2018).

In addition to lignin stemming from well-established and highly developed paper and pulp industry, another important source of technical lignin is alkaline lignin derived from alkaline pretreatment/fractionation of lignocellulosic biomass, which takes place under milder conditions as compared to soda process (Kim et al., 2016). The commonly applied reagents in alkaline pretreatment include sodium hydroxide (NaOH), sodium carbonate (Na_2CO_3), aqueous ammonia, anhydrous ammonia and lime ($Ca(OH)_2$) (Kim et al., 2016). Hydrolysis lignin, known as the by-product generated from the acid hydrolysis pretreatment process of lignocellulosic ethanol production, is another type of technical lignin that receives extensive investigation. It is usually separated from the stream before fermentation of cellulose derived saccharide (e.g. hexose and pentose) and is burnt for energy recovery (Li & Takkellapati, 2018).

Table 2.1 Commercial lignin production. Adapted from (Schutyser et al., 2018; Wang et al., 2019)

Lignin type	Sources	Production (kt/yr)	Features
Lignosulfonate (LS)	Sulfite pulping	≈1000	Oligomers with highly condensed structures and sulfonate (-SO_3) group (4-8 wt% S), low purity
Kraft lignin (KL)	Kraft pulping	≈90	Oligomers with highly condensed structures and thiol (-HS) group (1.5-3 wt% S), low purity
Soda lignin (SL)	Soda pulping	5-10	Sulfur free, oligomers, low purity
Organosolv lignin (OSL)	Organosolv pulping	≈3	Sulfur free, relatively high purity

2.2. Various Lignin Depolymerization Technologies

In the past few years, depolymerization of isolated lignin has become an extensively investigated research topic, resulting in a large number of depolymerization studies. In general, the various types of lignin depolymerization technologies can be roughly divided into three categories, biological, thermal, and chemical depolymerization (Xu et al., 2014). These categories can be further divided into several subsets in the literature, usually depending on the process characteristics such as reaction conditions, solvent and catalyst selection.

Biological depolymerization of lignin refers to the process of lignin degradation with the assistance of bacteria, fungi or isolated enzymes under relatively mild conditions. Enzymatic depolymerization is somehow overlapping with fungi and bacteria-assisted depolymerization because many types of lignin-degrading enzymes isolated from fungi and bacteria are implemented for *in vitro* conversion of lignin (Chen & Wan, 2017). Therefore, biological depolymerization of lignin can be fundamentally considered as enzyme-assisted degradation in either *vivo* or *vitro* conditions. Biological depolymerization not only exhibits high specificity and cost-effectiveness, but also poor productivity and low yield, which hinders its industrial application.

Thermal depolymerization routes usually require relatively harsh conditions and intensive energy input, making it less economically viable and environmentally friendly. Pyrolysis has received great interest as one of the baseline technologies for thermal depolymerization of lignin, which refers to the heating treatment of lignin at relatively high temperatures (400-600℃ or even higher) under anoxic conditions, with or without catalysts. In accordance with different heating rate and residence time, pyrolysis can be classified into conventional (or slow) pyrolysis and flash (or fast) pyrolysis (Laurichesse & Avérous, 2014). As another baseline technology of thermal depolymerization, hydrothermal liquefaction (HTL) is a better candidate for biomass with high water content because there is no need for preliminary drying processes, which is both energy-intensive and costly. HTL of lignin is usually carried out in hot-compressed subcritical water (≤ 374℃ and 22MPa), which has a few special properties such as low viscosity and high solubility of organic compounds, making it a good reaction medium for biomass conversion (Kumar et al., 2017).

Chemical depolymerization methods, which take advantages of different chemicals and reagents, are characterized as having a better control over the reaction and high product selectivity. It can be further divided into several subsets such as reductive depolymerization/hydrogenolysis,

oxidative depolymerization, homogeneous base/acid catalyzed depolymerization, and heterogeneous catalyzed depolymerization. In order to accelerate the biomass conversion rate and suppress the formation of undesirable product (e.g., char) while keeping the reaction conditions relatively mild, chemical depolymerization of lignin is often carried out in a combination with thermal techniques, namely thermochemical depolymerization.

2.3. Microwave Irradiation: An Energy-efficient Heating Method

2.3.1. Fundamentals of Microwave Irradiation

Microwaves are high-energy electromagnetic waves with frequencies ranging from 300MHz to 300GHz, corresponding to wavelengths varying from 1m to 1mm (Wang et al., 2016). In our daily lives, microwaves are usually tuned to a frequency (generally 2.45 GHz) to which molecules of water go into a vibrant dance, flipping back and forth 2.45 billion times per second. Three potential ways by which microwave and matter interaction include (1) absorption, (2) transmission, and (3) reflection, or any combination of these interactions. Accordingly, materials subjected to microwave irradiation can be roughly divided into three categories: (1) microwave absorbers (e.g. water and ethanol), where the microwaves can be absorbed by the material, resulting in rapid heating; (2) microwave-transparent material (e.g. quartz), where microwaves pass through without any losses; and (3) microwave-reflective material (e.g. metals), where microwaves cannot penetrate and are reflected (Asomaning et al., 2018).

When microwaves penetrate into organic molecules, the constantly fluctuating electromagnetic field leads to extreme oscillation and realignment of dipoles as well as the migration of ions in polar liquid. Consequently, friction is created inside of the material as the source of internal energy, which causes the bulk of the material to be heated up (Bundhoo, 2018). As a sub-category of dielectric heating, the energy conversion efficiency of microwave heating depends on the dielectric properties of the material. The dielectric properties of a material are determined by the material's ability to be polarized in an electric field and to store electric energy (known as dielectric constant ε'), and the material's ability to convert electrical energy into heat (known as dielectric loss ε'') (Aguilar-Reynosa et al., 2017; Asomaning et al., 2018). The quotient of these two parameters defines the dielectric loss tangent ($\tan \delta = \varepsilon'/ \varepsilon''$) or dissipation factor of a material, which refers to the ability of a material to convert electromagnetic (or microwave) energy into thermal energy at a certain temperature and frequency (Aguilar-Reynosa et al., 2017). Substances with high value of loss tangent ($\tan \delta > 0.5$) are identified as good microwave receptors

while substances with low value of loss tangent (tan $\delta < 0.1$) are considered as poor microwave absorbers (Asomaning et al., 2018). In comparison with non-polar solvent (e.g. hexane and toluene), polar solvent (e.g. ethanol and methanol) with higher loss tangent will preferentially absorb considerable microwave energy, which results in more molecular polarity orientation in free radical reaction and therefore remarkably improves the reaction rate (Wang et al., 2016).

2.3.2. Comparison of Microware and Conventional Heating

In comparison with conventional heating, MW heating exhibits a series of advantages. First of all, MW heating is characterized as non-contact heating as opposed to conventional heating because microwaves directly heat up the material inside the heating container instead of heating the walls of the container, resulting in less energy loss (Bundhoo, 2018). In addition, the temperature distribution of the reaction material during conventional heating and MW heating is completely opposite. The temperature at the center of the material subjected to MW irradiation is always higher than the temperature on the outer surface. On the contrary, during conventional heating the reaction material is heated through conduction or convection, leading to a lower "core" temperature (Miura et al., 2004). The detailed comparison of MW heating and conventional heating is presented in Table 2.2.

Table 2.2 Comparison between microwave heating and conventional heating. Adapted from (Bundhoo, 2018)

Microwave heating	Conventional heating	Remarks
Non-contact heating	Contact heating	With non-contact heating, the subject material is heated directly as opposed to conventional heating where the contained wall is heated more.
Lower energy consumption	Higher energy consumption	Although MW irradiation is not 100% energy efficient (energy loss during conversion of electrical energy into microwaves), it is less energy-consuming than conventional heating. This is due to considerable energy that is required for heating the container wall prior to heat the subject materials under conventional heating.
Rapid heating	Slow heating	Microwave energy is directly absorbed by subject material and transferred as heat, resulting in rapid heating. During conventional heating, the subject material is heated by convective heat transfer from reactor wall to subject material, and by conduction from the material surface to the material core.
Shorter reaction time	Longer reaction time	MW irradiation yield similar or higher quality products in shorter reaction times as opposed to conventional heating.
Volumetric heating	Superficial heating	Volumetric heating ensures uniform heat distribution in the material unlike superficial heating which occurs at the surface.
Higher level of control	Lower level of control	MW heating can be immediately switched on and off, and the energy applied to the material can be more precisely pre-determined based on per unit weight or volume basis.
Improved product yields	Lower product yields	Owing to the mechanism of MW heating, better product yields have been obtained as opposed to conventional heating.

2.4. Microwave-assisted Lignin Depolymerization

Due to the advantages over conventional heating, MW heating has been experimented to intensify lignin depolymerization processes through MW-assisted pyrolysis under relatively high temperature (＞400 ℃) and MW-assisted solvolysis/liquefaction under relatively mild conditions (usually＜200 ℃) (Dhar & Vinu, 2017; Wang et al., 2016).

As previously mentioned, pyrolysis has been commonly carried out under conventional heating. With MW heating gaining increasing attention over the past decade, MW heating has been considered as a heating method enhancing the pyrolytic process. Different from MW-assisted solvolysis that takes the advantage of a liquid solvent system as the media for biomass conversion, MW-assisted pyrolysis usually requires a MW-absorber to initiate and enhance the pyrolysis process as many types of biomass exhibit poor dielectric properties, resulting in low MW absorption (Bundhoo, 2018). The commonly employed MW-absorbers include carbon materials, metal, metal oxides and metal hydroxides (Li et al., 2016; Yin, 2012). Different operating parameters have been reported to influence the yield, distribution and quality of pyrolysis products, such as MW heating conditions (e.g. temperature, retention time, power setting, and reactor), characteristics of feedstocks (e.g. particle size and moisture content), MW-absorber selection, as well as catalysts used (Huang et al., 2016; Motasemi & Afzal, 2013).

In addition to MW-assisted pyrolysis, MW-assisted lignin solvolysis attracted much attention in recent years as well because it provides a relatively mild reaction environment and a single-phase condition due to the miscibility of organic products in the solvent (Duan et al., 2018). The current research interests of the scientific community mainly focus on the optimization of reaction conditions, solvent selection, catalyst screening, as well as the possible separation of obtained products. A summary of MW-assisted solvolysis of lignin under different reaction conditions is provided in Table 2.3.

Table 2.3 A summary of the salient results of existing studies on microwave-assisted solvolysis of lignin.

Feedstock	Reaction conditions	Solvent	Catalyst	Bio-oil Yield	Phenolic monomer yield	Reference
Wheat straw alkali lignin (0.57% ash content)	MW heating (800W), 100-180℃, 10-60min	Ethanol alone, FA alone, or ethanol/FA (1:3,v/v) cosolvent	Ferric sulfate	Not reported	≈20% (ethanol/FA cosolvent) ≈15% (FA solvent) ≈4% (ethanol solvent)	(Ouyang et al., 2015)
Wheat straw lignin	MW heating (300W) or conventional heating, 100-180℃, 10-60min	Ethylene glycol solvent 0-10 wt% phenol as hydrogen donor reagent	5-15 wt% sulfuric acid as catalyst	>95% (MW heating)	0.92% (conventional heating) 13.61% (MW heating)	(Ouyang et al., 2015)
Bamboo organosolv lignin	MW heating (<80W), 160℃, 30min	Ethanol	Sulfuric acid, hydrochloric acid, phosphoric acid, or formic acid	>90% (sulfuric acid)	Not reported	(Tayier et al., 2018)
Bamboo organosolv lignin (M_w~1579)	MW heating, 140-200℃, 30min	Ethanol/FA (1:1,v/v) cosolvent	Bamboo biochar supported Fe-600, Fe-800, Ni-600, Ni-800 catalysts	85% (200℃, Ni-600)	Not reported	(Tayier et al., 2020)
Akali lignin (M_w~2473)	MW heating (600W), 100-140℃; 20-80min	Ethylene glycol (EG), dimethyl sulfoxide (DMSO) and dimethyl formamide (DMF) solvents	No	Not reported	13.37% (DMSO, 60min, 100℃) 7.24% (EG, 60min, 100℃) 7.95 % (DMF, 60min, 120℃)	(Dhar & Vinu, 2017)
Black liquor lignin	MW heating (600W), 100-180℃, 5-60min	Isopropanol	No	43.45%	Not reported	(Liu et al., 2017)
Alkaline lignin (2.16% ash content, M_w~3260)	MW heating (400W) or conventional heating, 120-180℃, 15-45min	Methanol/FA cosolvent	No	41.1% (conventional heating) 72% (MW heating)	0.89% (conventional heating) 6.7% (MW heating)	(Shao et al., 2018)
Organolsov olive tree pruning lignin (0.39% ash content, M_w~7232)	MW heating (400W), 140℃, 30min	Tetralin or FA	Al-SBA-15 (Ni, Pd, or Ru)	17% (tetralin, Ni-Al-SBA) 30% (FA, Ni-Al-SBA)	0.42% (tetralin, Ni-Al-SBA) 0.618% (FA, Ni-Al-SBA)	(Toledano et al., 2014)
Organolsov olive tree pruning lignin (0.39% ash content, M_w~7232)	MW heating, 150℃, 30min	Tetralin, isopropanol, glycerol or FA	Ni10%Al-SBA-15	50% (isopropanol without catalyst) 30% (FA with catalyst)	0.07% (isopropanol without catalyst) 0.61% (FA with catalyst) 0.6% (FA without catalyst)	(Toledano et al., 2013)

				22% (FA without catalyst)		
Olive tree organosolv lignin (Fraction 1 to 6 derived from ultrafiltration with a descending order of M_w from 12798 to 4527)	MW heating (100W), 150°C, 30min	FA	Ni10%Al-SBA-15	Not reported	0.619%, 0.723%, 0.271%, 0.53%, 0.338% and 0.387% (lignin based) simple phenolic compounds derived from extracted lignin fraction 1, 2, 3, 4, 5, and 6 respectively	(Toledano et al., 2013)
Biolignin (BL), Eucalyptus lignin (EL), Harwood lignin (HL)	MW heating (400W), 180°C, 1h	FA	NiO/H-ZSM-5 zeolites	20% (3.5% NiO, HL) 12% (3.5% NiO, EL)	8.5% (3.5% NiO, HL) 7.4% (3.5% NiO, EL)	(Milovanović et al., 2016)
Black liquor lignin	MW heating (600W), 130°C, 30min	FA	HUSY catalyst modified by oxalic acid	88.28%	Not reported	(Shen et al., 2015)
Black liquor lignin	MW heating, (600W), 110-180°C, 5-90min	FA	No	64.08% (160°C,30min)	Not reported	(Dong et al., 2014; Wang et al., 2017)
Bamboo organosolv lignin (0.3% ash)	MW heating (100W), 160°C, 30min	Alcohol solvents (methanol, ethanol, butanol, ethanediol and isopropanol)	Sulfuric acid	27-84.9%	Not reported	(Duan et al., 2018)
Bamboo lignin (M_W~1597)	MW heating, 160°C, 30min	Ethanol/formic acid/hydrochloric acid cosolvent (2:1:1,v/v/v)	Metal chloride catalysts ($MgCl_2$, $AlCl_3$, $ZnCl_2$, and $MnCl_2$)	62.53% (without catalyst) 73.65% ($MnCl_2$)	36.6% including 16.94% G-type monomers, 8.76% S-type monomers and 10.9% H-type monomers	(Zou et al., 2018)
Alkaline lignin	MW heating (400W), 100-160°C, 40-80min	Methanol	CuNiAl based catalyst with different metal ratios	60.1% (160°C, 80min, metal ratio of 1.5:4.5:2)	Not reported	(Zhou et al., 2018)
Alkaline, de-alkaline lignin, and lignosulfonate	MW heating (400W), 140 or 160 °C in methanol; 160 or 180 °C in ethanol or isopropanol, 80min	Methanol, ethanol, or isopropanol	HSZ based HSZ-640 (Si/Al=18), HSZ-660 (Si/Al=30), HSZ-690 (Si/Al=240) catalysts	57.4% (alkaline lignin) 82.9% (de-alkaline lignin) 70.9% (lignosulfonate)	Not reported	(Zhou et al., 2019)

Based on the reported studies, it is widely agreed that temperature is one of the most important operating parameters that have a significant effect on the process of MW-assisted lignin depolymerization. Since lignin is structurally complex and thermally stable, adequate thermal energy is required for an efficient bond cleavage and decomposition of the condensed structure. Dong et al. (2014) investigated the effects of temperature on the product yield and distribution of phenolic compounds derived from MW-assisted depolymerization of black liquor lignin in formic acid at a temperature ranging from 110 to 180 ℃. The results indicated that the yield of bio-oil increased when the temperature was below 160 ℃. However, when the temperature reached 180 ℃, the yield of bio-oil surprisingly decreased. The observation shows that the repolymerization (or condensation) of lignin derived phenolic fragments could be promoted simultaneously by the increased temperature (Dong et al., 2014). Similar result was reported by Liu and coworkers (2017) that the decrease in bio-oil yield and the formation of undesirable product (e.g. bio-char) could be attributed to the repolymerization of liquid product under higher reaction temperatures.

The retention time is another important parameter affecting MW-assisted lignin depolymerization, resulting in different product distribution and depolymerization efficiency. In most cases, a modest increase in retention time will contribute to a higher product yield and a favorable conversion rate. But similar to the “backfire” of excessively increasing temperature, research has shown that a prolonged retention time would probably promote the re-condensation of degraded lignin fragments (Dong et al., 2014; Liu et al., 2017).

Solvent selection also plays an indispensable role in the process of lignin depolymerization. The most frequently investigated solvents include alcohols (e.g. methanol, ethanol and isopropanol) , carboxylic acids (e.g. formic acid), ethers (e.g. polyethylene glycol) as well as water binary solvent systems. Duan et al (2018). carried out a comparative study on lignin depolymerization under MW heating in various alcohol solvents (methanol, ethanol, butanol, ethanediol and isopropanol) and concluded that ethanol and methanol induced more bond cleavage in lignin structure, resulting in a higher yield of bio-oil (over 84%) compared to other alcohols. This could be due to the fact that simple alcohols are conductive to provide higher permeability and fluidity in biomass conversion processes (Duan et al., 2018). Toledano et al. (2013) comparatively investigated MW-assisted depolymerization of organolsov olive tree pruning lignin in a series of different hydrogen-donating solvent (formic acid, tetralin, isopropanol and glycerol)

and reported that the product distribution and obtained phenolic monomers were remarkably dependent on the solvent selection. Compared to other hydrogen-donating solvents employed in the lignin depolymerization reaction, formic acid provided the highest yield of phenolic monomers and negligible amount of bio-char. This was likely attributed to the acidolysis of lignin, and the thermally driven decomposition of formic acid into carbon dioxide and active hydrogen, which provided a favorable hydrogenolytic environment for lignin depolymerization (Toledano et al., 2013). Dhar and Vinu (2017) studied MW-assisted depolymerization of alkali lignin in the presence of different organic solvents including ethylene glycol (EG), dimethyl sulfoxide (DMSO), and dimethyl formamide (DMF). Results have shown that high microwave absorbing solvents like EG (tan δ = 1.35) and DMSO (tan δ = 0.825) provided higher yield of phenolic monomers at a lower temperature, while medium microwave absorbing solvent like DMF (tan δ = 0.161) led to higher yield of phenolic monomers at a higher temperature.

Catalyst screening is of significance as well because catalysis has been regarded as an essential technique in lignin conversion process. The main advantages of catalytic lignin depolymerization are to accelerate the conversion and suppress the formation of undesirable product (e.g. bio-char) while keeping the reaction conditions relatively mild. On the other hand, catalysts are also used to promote selective bond cleavage and therefore lead to the generation of specific compounds or increase the ratio of desirable downstream products (Pandey & Kim, 2011). The catalysts mostly applied for MW-assisted lignin depolymerization can be categorized into homogeneous catalysts (e.g. acid/base catalysts and metal salts), and heterogeneous catalysts (e.g. supported metal catalysts, mesoporous acidic aluminosilicate (Al-SBA-15) based catalysts and microporous HUSY based catalysts). Tayier et al. (2018) studied the catalytic effects of various acid (formic acid, sulfuric acid, hydrochloric acid and phosphoric acid) on the depolymerization of bamboo organolsov lignin under mild microwave heating and reported that sulfuric acid exhibited better catalytic performance on lignin depolymerization. Similar result was reported by Ouyang et al. (2015) that strong acidic condition was favorable for ether linkage breakage in lignin structure and contributed to higher yield of phenolic monomers. In the currently available literature, formic acid was employed not only as a solvent (or reaction media) as previously mentioned but also served as an acid “catalyst” in the lignin depolymerization processes in many studies using conventional heating sources (Ghoreishi et al., 2019b, 2019a; Huang et al., 2014; Huang et al., 2017; Kleinert et al., 2009; Oregui-Bengoechea et al., 2017). Oregui-Bengoechea et al. (2017)

firstly reported the subtle role that formic acid played in lignin depolymerization. They confirmed that formic acid did not merely served as an *in situ* hydrogen source but also reacted with lignin through a formylation-elimination-hydrogenolysis mechanism that resulted in depolymerization of lignin biopolymer. Zou et al. (2018) investigated the MW-assisted depolymerization of bamboo lignin with different metal chloride catalysts ($ZnCl_2$, $MgCl_2$, $AlCl_3$, $FeCl_3$ and $MnCl_2$) and found that $MnCl_2$ displayed a much higher catalytic capability to produce the highest yield of bio-oil (73.65%) and phenolic monomers (36.6%). Toledano and coworkers (2014) prepared a series of mesoporous Al-SBA-15 supported metal based catalysts such as nickel (2, 5 and 10 wt.%), palladium (2 wt.%), platinum (2 wt.%) and ruthenium (2 wt.%), and evaluated their catalytic performance during mild MW-assisted lignin depolymerization. Results had shown that Ni10%AlSBA provided the optimum degree of lignin depolymerization among all catalysts of interest and remarkably minimized the repolymerization phenomena (Toledano et al., 2014). Zhou et al. (2018) studied MW-assisted depolymerization of alkaline lignin in the presence of CuNiAl hydrotalcite based solid base catalysts and concluded that the metal ratio of 1.5:4.5:2 contributed to the highest yield of bio-oil.

2.5. Conclusions and Knowledge Gaps

It is undeniable that considerable efforts and progresses have been made in the past decades for the enhancement of lignocellulosic biorefinery industry. However, there are still some knowledge gaps in the development of lignin depolymerization for value-added product production. Based on the comprehensive review of literature, one of the biggest knowledge gaps in the field of lignin depolymerization is that the currently available studies generally report various quantitative measures, such as BO yield, PM yield, total product yield, lignin conversion rate, molecular weight of depolymerized lignin product, relative peak area percentage of phenolic compounds. These quantitative measures can be defined in various ways in the literature. In addition, a wide array of isolated lignins, which may differ substantially in terms of their chemical structure, molecular weight, and impurity profile, are used as the feedstocks of lignin depolymerization. The inconsistency in the literature often does not allow for a straightforward comparison of lignin depolymerization studies. For this reason, BO yield and PM yield are selected as two measures of depolymerization efficiency in this research.

On the other hand, the development of lignin depolymerization technologies is still in its infancy. Studies on MW-assisted solvolysis of lignin under mild conditions are relatively limited

in the literature. The current research interests mainly focus on the optimization of reaction conditions, solvent selection, catalyst screening, and possible fractionation of lignin-derived products. In terms of the optimization of reaction conditions, a large number of process variables have been explored in the literature such as temperature, retention time, heating rate, stirring speed, feedstock concentration, and reactor scale. However, inconsistent feedstock selection and downstream recovery methods led to a lot of confusing and conflicting results, which requires more efforts to develop more effective downstream processing protocols for lignin feedstocks of interest. In addition, most studies in the literature implemented the "one-factor-at-a-time" experimental design, which is not efficient and can be devastated by possibly existing interactions between different factors. Based on the Fisher's factorial concept, it is necessary to carry out statistically designed experiments (e.g. simple factorial design or higher-level response surface design) to study the factors of interest together for further process optimization. Regarding the solvent selection, various types of reaction solvent systems (e.g. single organic solvent or binary solvent system) have been intensively investigated, and ethanol was identified as one of the promising hydrogen-donating solvents for efficient lignin depolymerization. However, there are not much research presenting a comparison of the solvent effect between ethanol and water, which is the greenest solvent with a low cost and large availability. Therefore, it would be interesting to conduct a comparative study between ethanolic and aqueous solvent systems in terms of the yield and physicochemical properties of lignin-derived product. When it comes to catalyst screening, many studies use precious metal catalysts, which are costly and nearly nonrecyclable. The biomass-derived simple carboxylic acid, FA, has received greater interest in recent years as an *in situ* hydrogen donor or homogeneous acid catalyst in lignin depolymerization in comparison to heterogeneous noble metal-based catalysts, for the consideration of economic viability and environmental friendliness. Nevertheless, the roles (hydrogen donor/acid catalyst/reactant) that FA play in lignin conversion and the relevant reaction mechanisms are still not fully understood, which calls for further investigation to unravel this knowledge gap.

In this project, the above-mentioned challenges will be addressed. The outcomes from this research will help gain insights into critical process variables, optimize MW-assisted lignin depolymerization, improve downstream recovery of desired products, and better understand the solvent effects on lignin conversion.

Chapter 3: Materials and Methods

The purpose of this chapter is to describe the basic materials, experiment setup procedures for the MW-assisted lignin depolymerization, product separation procedures, as well as the methods for feedstock and product characterization.

3.1. Materials

Alkaline lignin (product number: L0082) and de-alkaline lignin (product number: L0045) purchased from Tokyo Chemical Industry Co., Ltd. (TCI) were selected as the biomass feedstocks of MW-assisted lignin depolymerization. The solvents used during lignin depolymerization were anhydrous alcohol and reagent grade formic acid (≥95%) purchased from VWR International Ltd. and Sigma Aldrich Ltd., respectively. Other solvents and chemicals include ACS reagent grade hexane, inhibitor-free tetrahydrofuran (THF) (>99.9%), naphthalene D8 (internal standard), anhydrous sodium sulphate (Na_2SO_4), and N-Methyl-N-(trimethylsilyl)-trifluoroacetamide (MSTFA) for GC derivatization (≥98.5%) purchased from Sigma Aldrich Ltd. All chemicals were used as received.

3.2. Lignin depolymerization in Microwave Reactor

MW-assisted lignin depolymerization was carried out in a Multi-wave PRO microwave reactor equipped with a digital control system (as shown in Fig. 3.1) from Anton Parr GmbH (Graz, Austria). In a typical run, a magnetic rotor was loaded into the quartz vessel (80ml) before the reaction was initiated to prevent the hotspot problem, followed by an addition of lignin powder, ethanol and formic acid (FA) with a designated lignin concentration and FA/lignin mass ratio. Lignin concentration was defined as the mass of lignin feedstock divided by the total mass of reactants including lignin feedstock, reaction solvent and FA, and multiplied by 100%. The mixture was oscillated mildly to reduce suspensions and improve mixing. With all preparations completed, the mixture was heated up to a preset temperature at a constant heating rate (10°C/min). When the temperature reached the pre-set value, the reaction temperature within the reactor remained unchanged for a certain time period, termed retention time, by automatic power adjustment. Once the reaction was completed, the sample was cooled down to room temperature for further downstream processing. For each condition, the experiments were conducted in duplicate and the results were presented using mean values.

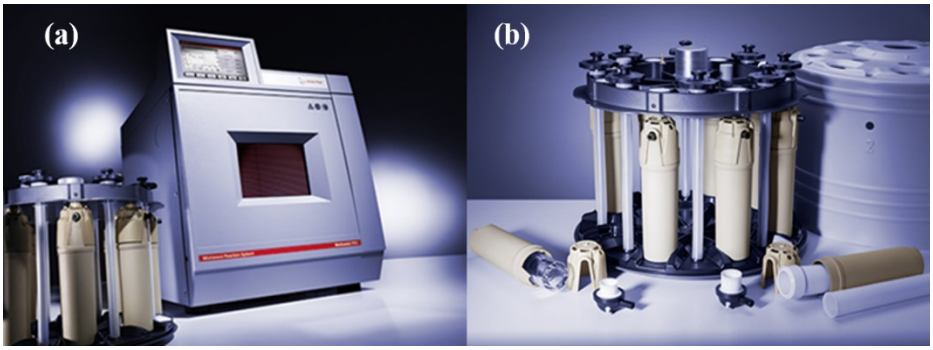

Figure 3.1 Microwave reactor (a) and multi-position modular platform system (b)

3.3. Separation of Reaction Products

Fig. 3.2 shows the schematic representation of product separation procedures. After the reaction was completed, the cooled reactor was opened without collecting gaseous product. Since the main focus of this study was lignin-derived bio-oil (BO) and phenolic monomers (PM), gas fraction was thus not collected and analyzed in this work. The mixture post reaction was poured into a beaker and filtered through a pre-weighed Whatman No. 5 filter paper (2.5μm) under reduced pressure to separate liquid product from solid residue. Then the inner wall of quartz vessel was rinsed with ethanol several times to remove any leftover matter including adhering bio-oil and solid residue. Afterwards, the mixture containing ethanol-dissolved organic phase and solid residue was filtered through the same filter paper. The remaining solids on the filter paper were dried in an oven at 105℃ for 12h and then weighed to determine the yield of solid residue. The liquid product was dried over 2g anhydrous sodium sulphate (Na_2SO_4) to remove possibly existing water content, filtered through a Whatman PTFE membrane syringe filter (0.45μm) afterwards, and concentrated at 70℃ by using a Organomation nitrogen evaporator (N-EVAP 112) to remove ethanol and obtain bio-oil. Ethanol was considered to be completely evaporated when the mass change of bio-oil during the 10-minute evaporation interval was less than 0.01g. The yields of bio-oil (BO) was determined on a dry ash free (DAF) basis and the yield of solid residue (SR) was determined on a dry basis by the following equations.

$$\text{Yield of BO (wt\%)} = \frac{Mass\ of\ BO}{Mass\ of\ DAF\ lignin} \times 100\%$$

$$\text{Yield of SR (wt\%)} = \frac{Mass\ of\ SR}{Mass\ of\ dry\ lignin} \times 100\%$$

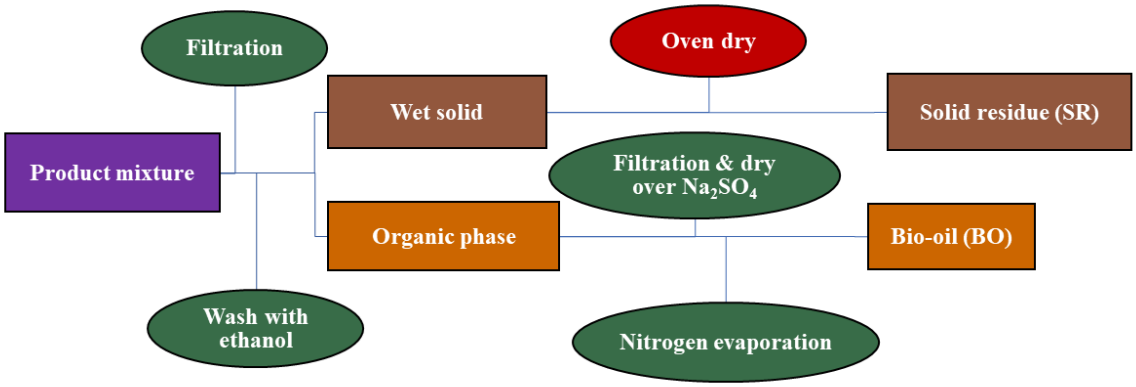

Figure 3.2 Schematic representation of separation procedures

3.4. Feedstock Characterization

Table 3.1 shows the product specifications provided by the supplier (TCI), alkaline lignin is prepared from de-alkaline lignin by adjusting the pH value from acidic range to alkaline range. The pH level of TCI alkaline lignin at a concentration of 50g/L and a temperature 25℃ is around 8.0 to 10.0 while that of de-alkaline lignin is around 3.0 to 4.0. In terms of the structural characteristics of lignin feedstocks, alkaline and de-alkaline lignin have similar amount of methoxy group, sulfo group and carboxy group.

Table 3.1 Specifications of lignin feedstocks provided by TCI

Test	Lignin feedstock	
	Alkaline lignin	De-alkaline lignin
pH	8.0-10.0 (50g/L, 25℃)	3.0-4.0 (50g/L, 25℃)
Methoxy group	10-12% (dry basis)	10-12.5% (dry basis)
Sulfo group	Similar between two types of lignin feedstocks	
Carboxy group	Similar between two types of lignin feedstocks	

Table 3.2 presents the result of inductively coupled plasma (ICP) mineral content analysis provided by SGS Agri-Food Laboratories. The analytical results revealed the presence of sodium in both alkaline and de-alkaline lignin. This observation could be explained by the product preparation information provided by the supplier (TCI company) that both types of lignin feedstock were prepared from sodium lignosulfonate (LS) yielded from the sulfite process, wherein sodium sulfite (Na_2SO_3) is typically used as the reagent.

Table 3.2 ICP mineral analysis on two types of lignin feedstocks

Test	Lignin feedstock	
	Alkaline lignin	De-alkaline lignin
Sodium (Na)	4.30%	4.38%
Potassium (K)	<0.00%	0.02%
Magnesium (Mg)	<0.00%	0.03%
Calcium (Ca)	<0.00%	<0.00%
Phosphorus (P)	<0.00%	<0.00%

Table 3.2 shows the composition of two types of lignin feedstocks. The moisture content of lignin feedstocks was testing by drying the sample with an oven at 105℃ for over 12h, based on ASTM E1756. The moisture content of de-alkaline lignin (11.44%) is higher than that of alkaline lignin (6.26%). In terms of the ash content of lignin feedstocks tested by using a muffle furnace, alkaline lignin contained a significantly larger amount of ash (58.00%) than de-alkaline lignin (13.90%) when the standard test method for ash content in biomass (ASTM E1755) was applied. However, oxidation of alkaline lignin samples at 575℃ by following the ASTM E1755 resulted in dark-colored ash as shown in Fig. 3.2 (a), indicating that organic carbon compounds were not completely removed. In light of this, the standard test method for ash content in petroleum product (ASTM D482) with a higher temperature (775℃) was applied, leading to light-colored alkaline lignin ash as shown in Fig. 3.2 (b). Overall, ashing the alkaline lignin sample at 775℃ yielded a considerably lower amount of ash than 575℃ (58.00% vs. 15.51%), while only negligible changes in de-alkaline lignin ash content was observed (13.90% vs. 13.85%). This suggested that alkaline lignin might contain a great amount of rigid organic carbon compounds which can only be removed under harsh conditions, as opposed to its counterpart. Therefore, we considered the standard test method for ash content in petroleum product (ASTM D482) to be a better approach for ash content determination in our study as it is reproducible and ensures the complete removal of organic carbon compounds. More specifically, the ash contents of alkaline and de-alkaline lignin are 15.51% and 13.85% respectively, based on the original mass of samples.

Table 3.3 Composition of lignin feedstocks

Lignin feedstock	Moisture content	Ash content [a]	Ash content [b]
Alkaline lignin	6.26%	58.00%	15.51%
De-alkaline lignin	11.44%	13.90%	13.85%

Notes: [a]: based on ASTM E1755 for ash content in biomass at 575℃; [b]: based on ASTM D482 for ash content in petroleum product at 775℃; All results are reported relative to the original mass of sample, not oven dried mass.

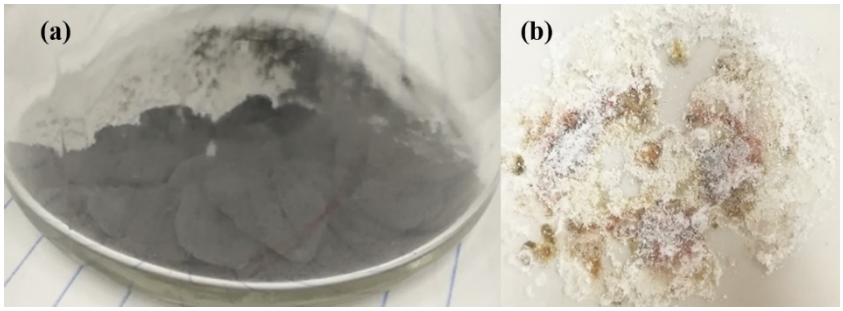

Figure 3.3 Alkaline lignin ash obtained from ASTM E1755 (a) and ASTM D482 (b)

3.5. Characterization of Bio-oil and Phenolic Monomers

The low-molecular-weight phenolic compounds in BO were analyzed qualitatively and quantitatively with a gas chromatograph-mass spectrometer (GC-MS). GC-MS analysis was carried out using a Perkin Elmer Clarus 680 GC coupled with a Clarus SQ8 MS. Approximately 20mg BO sample was carefully loaded into a 5mL volumetric flask, followed by an addition of 10μL internal standard solution (5000μg/mL naphthalene D8 in THF). A proper amount of THF (HPLC grade) was added into the 5mL volumetric flask, resulting in a sample solution consisting of around 10μg/mL internal standard and 4000μg/mL BO. The prepared sample solution was mildly oscillated and filtered through a 0.2μm syringe filter before being injected into GC-MS. GC-MS analysis was carried out using a Perkin Elmer Clarus 680 GC coupled with a Clarus SQ8 MS and a Raxi-5ms column (30m length*0.25mm internal diameter*0.25μm thickness). The injection volume was 1μL, and the GC injection port was operated at 280℃ in a split mode, with a split ratio of 10:1. Helium was used as the carrier gas, with a flow rate of 1mL/min. The oven temperature was initially set at 70℃ (held for 2 minutes), raised up to 250℃ at a heating rate of 10℃/min, then increased to 280℃ at a heating rate of 6℃/min, giving a total run time of 25 minutes. It is necessary to mention that in Chapter 6 and Chapter 7, silylation was performed to increase sample volatility and to better detect PM in BO samples. 500μL N-Methyl-N-(trimethylsilyl)-trifluoroacetamide (MSTFA) was mixed with 500μL BO sample solution (in THF) containing internal standard. The mixture was kept at room temperature for approximately 10min prior to GC-MS analysis. Based on the integrated peak area, thirty peaks (or chemical compounds) in total ion chromatography (TIC) were identified by using the NIST library, and were further quantified by the internal standard. The monomeric phenolic compounds were categorized into

three groups, including phenol (H) type, guaiacol (G) type and syringol (S) type that contain zero, one and two methoxyl groups (O-CH_3) respectively. The yield of phenolic monomers (PM) in bio-oil was determined on a dry ash free basis using the following equation.

$$\text{Yield of PM (wt\%)} = \frac{Mass\ of\ GCMS\ detectable\ PM}{Mass\ of\ DAF\ lignin} \times 100\%$$

The relative molecular mass M_n (number average molecular mass), M_w (weight average molecular mass), and polydispersity index (PDI=M_w/M_n) of the obtained BO were determined with a Waters Breeze gel permeation chromatography (GPC) instrument. The GPC instrument is equipped with a 1525 binary high-performance liquid chromatography (HPLC) pump, a UV detector at a wavelength of 270nm, as well as a Waters Styragel HR1 column. The column temperature was set as 40℃, and THF was used as the eluent with a flow rate of 1mL/min. The polystyrene standard was used for the calibration of sample molecular mass. Selected BO samples were mailed to the Institute for Chemical and Fuels from Alternative Resources (ICFAR) at Western University for GPC analysis. Since both types of lignin feedstocks are not soluble in THF, acetylation of lignin feedstocks with acetic anhydride/pyridine (1/1, v/v) at room temperature was carried out to enhance their solubility in organic solvent prior to GPC analysis. However, the low solubility of selected lignin feedstocks in acetic anhydride and pyridine led to unsatisfactory acetylation. Therefore, GPC analysis was not carried out to determine the relative molecular mass of lignin feedstocks.

3.6. Bio-oil Recovery by Ethyl Acetate-Water Extraction

Lignin was depolymerized in the MW reactor at a temperature of 230 °C, a retention time of 140 min with a feedstock concentration of 8% and a FA/DAF lignin mass ratio of 2 in the same manner as described in section 3.2. After the reaction was completed, the product mixture was filtered to separate liquid organic phase and SR. The pH level of the filtrate (organic phase) was adjusted to acidic level (pH=1), neutral level (pH=7), or basic level (pH=13) with 2M hydrochloric acid (HCl) solution or 2M sodium hydroxide (NaOH) solution prior to liquid-liquid extraction (LLE) of phenolic BO using both ethyl acetate and water as the extractants. In addition, an excessive amount of water was used to wash the organic phase containing phenolic BO to remove possibly existing impurities. The detailed stepwise description of the “in-house” downstream recovery method adapted in this study was presented Appendix 3.

3.7. Lignin Depolymerization in Aqueous Solvent System

Lignin depolymerization in aqueous solvent system is the same as described in Section 3.2. Separation of bio-oil follows the procedure described in Section 3.6.

Chapter 4: Investigation of the Impacts of Process Variables on Product Yields Using a Response Surface Methodology

Response surface methodology (RSM) is considered as a collection of mathematical and statistical techniques useful for modeling and analyzing problems in which a response of interest is affected by several variables and the objective is to optimize the response (Montgomery, 2017). In comparison to other experimental design methodologies, RSM exhibits the advantage of optimizing systems with imbedded curved relationships, and allowing a more precise computation of the main and interaction effects through regression fitting (Zhu et al., 2018). Central composite design (CCD), one of the most commonly used response surface design, is an upgraded factorial (or fractional factorial) design with center points, augmented with axial points (also known as star points) (Hanrahan & Lu, 2006). A CCD can be used to effectively estimate first-order terms and second-order terms. In addition, it is especially useful in sequential experiment since researchers can model the response variable with curved relationships by adding center points and axial points to a previously done factorial (or fractional factorial) design (Montgomery, 2017).

Two types of lignin feedstocks, alkaline and de-alkaline lignin, were selected as the raw materials for this study on lignin depolymerization. Based on the comprehensive literature review, four independent variables were considered as critical in the process of MW-assisted lignin depolymerization, including feedstock concentration, FA to feedstock mass ratio, temperature, and retention time. Therefore, this chapter aims to investigate the influence of these four factors on the yield of BO and PM generated from either alkaline or de-alkaline lignin using a response surface design.

4.1. Test for Curvature

Checking for curved relationships between factors of interest and the responses is an important step before we proceed to a more complicated response surface design and to further explore the influences of factors on the responses. The general 2^k factorial design does not allow a test for curvature because 2^k factorial designs, in which each factor only has two levels, assume there is a linear relationship between each factor and the response. Therefore, the method of adding replicating center point to the 2^k factorial design (corner points) was applied to obtain an estimate of error, and more importantly, check for quadratic effects (curvature) in the fitted data. As the name implies, center points are experimental runs where the level of factors are set halfway between the low and high settings. The test for curvature compares the fitted mean of the response

at center points with the expected mean if there are linear relationships between model terms and the response. In simple terms, the curvature is statistically significant when the center points are far away from the linear that joins the means of the corner points. Conversely, the curvature is not statistically significant when the center points are lying on or close to the line that joins the means of the corner points (Montgomery, 2017).

With the addition of replicating center points, a 2^k factorial design involving four factors of interest, namely feedstock concentration (10 wt.% vs. 20 wt.%), FA to feedstock mass ratio (0.5 vs. 1.5), temperature (170℃ vs. 230℃), and retention time (60min vs. 140min), was applied to evaluate their relationships (linearity or curvature) with the responses in MW-assisted lignin depolymerization, as shown in Table 4.1. The yields of bio-oil (BO) and phenolic monomers (PM) derived from alkaline and de-alkaline lignin were selected as the responses. The obtained p-values for curvature from ANOVA were presented in Table 4.2. It can be clearly observed that most of the p-values for curvature were significant (p-value = 0.000), and only a near-marginal significance was observed ($0.05 < \text{p-value} = 0.064 < 0.1$) when the response was the yield of bio-oil (BO) derived from de-alkaline lignin. In other words, at least one factor of interest has a curved relationship with the response, suggesting that we should proceed to a response surface design to model the curvature and to further investigate the effects of factors on the responses.

Table 4.1 Factors and levels used for the 2^k factorial design

Factors	Levels	Low setting	High setting
Feedstock concentration (%)	2	10	20
FA/feedstock mass ratio	2	0.5	1.5
Temperature (℃)	2	170	230
Retention time (min)	2	60	140

Table 4.2 Analysis of variance (ANOVA) p-values for curvature test. Significant and marginally significant p-values for curvature are shown in bold.

Reponses	A BO	A PM	D BO	D PM
p-values for curvature	**0.000**	**0.000**	**0.064**	**0.004**

Notes: $0.05 < \text{p-value} < 0.1$ denoted to marginal significance; p-value < 0.05 denotes significance; A BO = alkaline lignin BO yield; A PM = alkaline lignin PM yield; D BO = de-alkaline lignin BO yield; D PM = de-alkaline lignin PM yield

4.2. Central Composite Design

Based on the previous conclusion that at least one of the factors of interest has a curved relationship with the response, a 3-level-4-factor CCD of RSM was applied to study the effect of

process variables on product yields within the experimental range. Four process variables of interest are feedstock concentration (X_1), FA to feedstock mass ratio (X_2), temperature (X_3), and retention time (X_4) at three coded levels (-1, 0, +1). The yields of BO and PM were selected as the responses. The alpha value was calculated by using the following equation,

$$\alpha = \sqrt[4]{2^n}$$

where, n refers to the number of factors. The ranges of process variables were selected based on the relevant study reported in the literature and the limitations of our experimental instruments. The feedstock concentration was evaluated within the range of 10 to 20 wt.%, the FA to feedstock mass ratio covered a range from 0.5 to 1.5, the temperature was set from 170 to 230℃, and the retention time was ranging from 60 to 140 min, as presented in Table 4.3. This design contained 31 experimental combinations, including 7 center points, 8 axial points and 16 factorial points. All of these combinations were duplicated, giving 62 experimental runs in total for each type of feedstock.

The complete design matrix of CCD and the corresponding response data (alkaline BO yield, de-alkaline BO yield, alkaline PM yield, de-alkaline PM yield) are listed in Table 4.4. As shown in Table 4.4, the BO yield derived from alkaline lignin varied between 12.20% and 70.63% while BO yield derived from de-alkaline lignin was ranging from 26.75% to 61.18%. The PM yield generated from alkaline lignin varied between 0.35% and 1.95% while PM yield generated from de-alkaline lignin was ranging from 1.56% to 2.56%.

Table 4.3 Process variables and coded levels of microwave-assisted lignin depolymerization

Factors	Symbol	Coded level		
		-1	0	+1
Feedstock concentration (%)	X_1	10	15	20
FA/feedstock mass ratio	X_2	0.5	1	1.5
Temperature (℃)	X_3	170	200	230
Retention time (min)	X_4	60	100	140

Table 4.4 The central composite design (CCD) of four independent variables and the corresponding experimental values of responses

	Conc (%)	FA Ratio	Temp (℃)	Time (min)	Alkaline lignin		De-alkaline lignin	
Run	X_1	X_2	X_3	X_4	BO yield	PM yield	BO yield	PM yield
1	10	0.5	170	60	32.43	1.72	42.43	2.03
2	20	0.5	170	60	26.86	1.51	36.11	1.89

3	10	1.5	170	60	42.94	1.50	50.72	2.01
4	20	1.5	170	60	50.47	1.41	48.70	2.12
5	10	0.5	230	60	15.52	0.87	32.25	1.92
6	20	0.5	230	60	20.62	0.80	26.75	1.61
7	10	1.5	230	60	42.46	1.23	45.44	2.24
8	20	1.5	230	60	67.23	1.63	58.89	2.40
9	10	0.5	170	140	29.29	1.50	42.70	2.02
10	20	0.5	170	140	19.21	1.95	38.49	1.89
11	10	1.5	170	140	53.42	0.35	53.86	2.12
12	20	1.5	170	140	54.87	1.40	54.93	2.17
13	10	0.5	230	140	12.20	0.97	28.29	1.78
14	20	0.5	230	140	20.66	1.09	27.55	1.56
15	10	1.5	230	140	40.71	1.77	48.57	2.28
16	20	1.5	230	140	70.63	1.51	61.18	2.56
17	10	1	200	100	33.80	1.29	45.21	2.11
18	20	1	200	100	43.74	1.39	36.70	1.71
19	15	0.5	200	100	16.75	0.87	35.20	2.01
20	15	1.5	200	100	50.87	0.91	52.83	2.23
21	15	1	170	100	33.57	1.41	46.43	2.00
22	15	1	230	100	29.03	1.07	38.10	1.68
23	15	1	200	60	31.88	1.09	43.63	2.20
24	15	1	200	140	23.43	0.63	47.59	2.15
25	15	1	200	100	22.80	0.94	45.62	2.25
26	15	1	200	100	26.34	0.88	45.96	2.16
27	15	1	200	100	26.01	0.85	46.50	2.23
28	15	1	200	100	26.50	0.90	43.84	2.07
29	15	1	200	100	25.16	1.12	46.86	2.25
30	15	1	200	100	27.07	0.80	45.54	2.05
31	15	1	200	100	26.45	0.90	43.76	2.13

Notes: Conc=feedstock concentration; FA ratio=FA to feedstock mass ratio; Temp=temperature; Time=retention time

4.3. Analysis of Variance

Based on the experimental data derived from CCD, ANOVA (Table 4.5) was carried out to explore the influence of feedstock concentration, FA to feedstock mass ratio, temperature, and retention time on BO and PM yield. From Table 4.5, all model terms with p-value<0.05 are significant, suggesting that the responses were interactive and complicated. A significant p-value

indicates that at least one mean is different from others within main (or linear) effects, square effects, or two-way interaction effects.

Table 4.5 Analysis of variance (ANOVA) F-values and p-values that show the significance of the main and interaction effects on BO yield and PM yield. Significant effects are shown in bold.

	A BO		A PM		D BO		D PM	
Source of variation	F-value	p-value	F-value	p-value	F-value	p-value	F-value	p-value
Linear								
X_1	22.75	**0.00**	2.57	0.13	0.00	0.99	1.28	0.27
X_2	336.79	**0.00**	0.21	0.66	224.19	**0.00**	39.04	**0.00**
X_3	2.70	0.12	3.89	0.07	18.39	**0.00**	0.16	0.69
X_4	0.11	0.75	0.40	0.53	2.73	0.12	0.03	0.86
Square								
X_1^2	14.03	**0.00**	6.82	**0.02**	2.46	0.14	2.18	0.16
X_2^2	2.30	0.15	0.51	0.49	0.11	0.75	1.21	0.29
X_3^2	0.15	0.70	3.43	0.08	0.58	0.46	5.57	**0.03**
X_4^2	1.56	0.23	0.85	0.37	1.72	0.21	3.39	0.08
Two-way interaction								
X_1X_2	28.03	**0.00**	0.87	0.37	16.18	**0.00**	7.19	**0.02**
X_1X_3	21.69	**0.00**	1.36	0.26	9.04	**0.01**	0.00	0.99
X_1X_4	0.05	0.83	2.35	0.14	0.77	0.39	0.09	0.77
X_2X_3	15.87	**0.00**	25.59	**0.00**	23.77	**0.00**	15.35	**0.00**
X_2X_4	4.86	**0.04**	2.40	0.14	2.17	0.16	1.16	0.30
X_3X_4	0.11	0.75	4.01	0.06	0.88	0.36	0.08	0.78

Notes: X_1=feedstock concentration; X_2=FA/feedstock mass ratio; X_3=temperature; X_4=retention time

4.3.1. Effects of Linear Terms

Regarding the linear terms, retention time is the only linear model term that did not have a significant effect on both BO and PM yield. Among four linear terms that exhibit significant results, FA/feedstock mass ratio has the most dominant influence on the responses, as evidenced by its higher F-values.

Fig. 4.1 shows the main effect plots of "FA/feedstock mass ratio" on BO yield derived from alkaline and de-alkaline lignin. It can be noted that an increase in FA/feedstock mass ratio from 0.5 to 1.5 led to a significant increase in BO yield derived from alkaline lignin, from around 15% to over 45%. Similar trend can be observed for the yield of BO derived from de-alkaline lignin.

As FA/feedstock mass ratio increased from 0.5 to 1.5, the corresponding yield of de-alkaline lignin BO yield substantially increased from 35% to roughly 55%. Based on the above observations, increases in FA to feedstock mass ratio played a positive role in lignin depolymerization, and therefore contributed to increases in product yields. This is understandable as formic acid has been recognized as an efficient "catalyst" for lignin depolymerization and has been well documented in many other studies (Huang et al., 2014; Kristianto et al., 2017; Park et al., 2016; Shao et al., 2018). The positive effects of FA in lignin depolymerization was likely due to the hydrogen donating property of FA and the active hydrogen generated from FA decomposition at high temperature, which helped to supress the repolymerization of the reactive intermediate products (Huang et al., 2014; Oregui-Bengoechea et al., 2017).

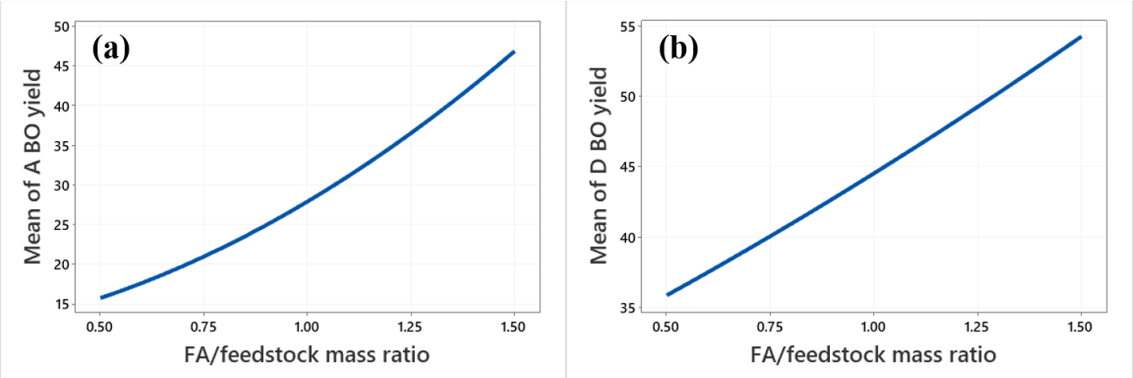

Figure 4.1 Main effect plot of "FA/feedstock mass ratio" on alkaline lignin BO yield (a) and de-alkaline lignin BO yield (b)

4.3.2. Effects of Interaction Model Terms

In terms of the interaction models terms, a few FA-involved 2-way interactions are regarded as the most significant interaction model terms on the responses, which re-emphasize that "FA/feedstock mass ratio" has the most dominant influence on product yields. For alkaline lignin, the 2-way interaction between "Feedstock concentration" and "FA/feedstock mass ratio" has the most significant interaction effect on BO yield while the interaction between "FA/feedstock mass ratio" and "Temperature" significantly affected PM yield. For de-alkaline lignin, the 2-way interaction of "FA/feedstock mass ratio*Temperature" was the most significant interaction effect on both BO and PM yields.

The three-dimensional response surface plots and contour plots for four responses of interest were plotted in Fig. 4.2 – Fig. 4.5, respectively. Since there were four factors of interest in this study, the interaction effect of two factors were investigated by keeping the other two factors

at a constant central point level. Contour lines connect points that have the same fitted response values, and colored contour bands represent the ranges of the fitted response values.

The interaction effect between "Feedstock concentration" and "FA/feedstock mass ratio" is show in Fig. 4.2. The color ramp of contour bands became darker as the predictor in y-axis increased, suggesting that the yield of BO derived from alkaline lignin remarkably increased with FA/feedstock mass ratio at a fixed feedstock concentration. This was likely due to the fact that FA can improve the BO yield by preventing lignin-derived intermediates from repolymerization during the reaction. Similar result was reported by Park et al. (2016) that the addition of FA led to an increasing yield of BO and a decreasing yield of bio-char in supercritical treatment of organosolv lignin in ethanol/FA cosolvent. In addition, the positive effect of FA seemed to become more outstanding when the feedstock concentration was at higher levels (above 16%). When the feedstock concentration was at its lowest setting (10%), the increase in FA loading resulted in an increase in BO yield from 24% to 47%. However, a more significant increasing trend of BO yield (from 24% to 63%) can be observed when FA/feedstock mass ratio was at its highest setting (20%). This observation suggested that the amount of FA required for efficient lignin depolymerization might be correlated with the total volume of liquid reaction media (varied with feedstock concentration) due to different concentrations of FA in the solvent system. A lower volume of liquid reaction media (or a higher feedstock concentration) likely contributed to a more efficient mass transfer of reactants and heat transfer during the reaction. Within the experimental range, higher yield of alkaline lignin BO (>50%) can be achieved when the feedstock concentration was higher than 16.5% and the FA/feedstock mass ratio was above 1.25.

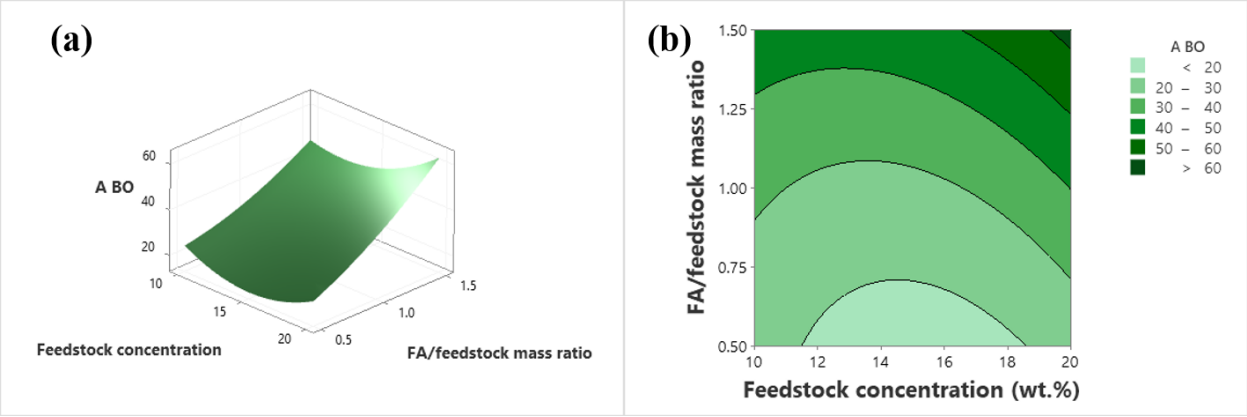

Figure 4.2 The response surface plot (a) and contour plot (b) for alkaline lignin BO yield as a function of feedstock concentration and FA/feedstock mass ratio.

Fig. 4.3 illustrates the interaction effect between “FA/feedstock mass ratio” and “Temperature” on the response of alkaline lignin PM yield. The yield of PM stemming from alkaline lignin gradually decreased with increasing temperature when the temperature was at low levels (below 200℃). However, we can clearly observe that the yield of alkaline lignin PM presented an increasing trend with a further increase in temperature (above 200℃). From the colored contour bands, it was worth noticing that lower temperature was favorable for maximizing the yield of alkaline lignin PM when the FA/feedstock mass ratio was low. Higher temperature was more suitable when the FA/feedstock mass ratio was high. This could be explained by the role of FA in lignin conversion processes. As reported by Oregui-Bengoechea et al. (2017), FA did not merely serve as a hydrogen donor but also seemed to react with lignin through a formylation-elimination-hydrogenolysis mechanism, leading to the depolymerization of lignin biopolymer and stabilization of lignin-derived fragments under the synergistic effect with ethanol solvent. The positive role that FA plays in stabilizing the reactive lignin-derived intermediates seems to intensely compete with the enhanced repolymerization reactions induced by excessively increasing temperature. Therefore, an increase in temperature might result in completely opposite effects on PM yield, depending on different levels of FA loading (FA/feedstock mass ratio). In other words, the amount of FA necessitated for effective lignin depolymerization was presumably interplay with the temperature due to the competition between thermally driven decomposition of FA that favors lignin depolymerization and the aggravated repolymerization of intermediates triggered by the increasing temperature. Within the experimental range, high yield of PM (>1.2%) derived from alkaline lignin can be achieved by the combination of lower temperature (<180℃) and lower FA/feedstock mass ratio (<1.2%), or the combination of higher temperature (>225℃) and higher feedstock concentration (>1.2%).

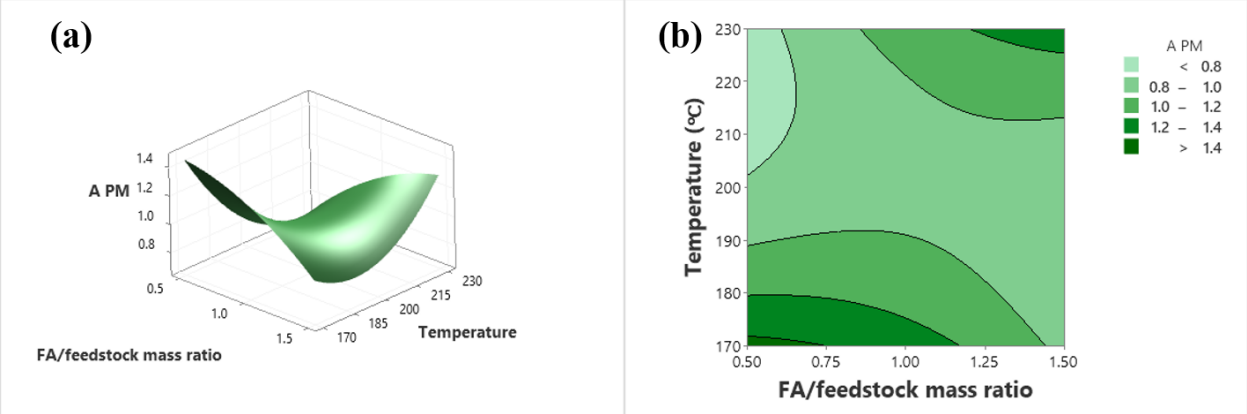

Figure 4.3 The response surface plot (a) and contour plot (b) for alkaline lignin PM yield as a function of FA/feedstock mass ratio and temperature

Fig. 4.4 depicts the interaction effect between "FA/feedstock mass ratio" and "Temperature" in response to the yield of BO derived from de-alkaline lignin, while holding "Feedstock concentration" and "Retention time" at constant values of 15% and 100min respectively. It can be observed that the de-alkaline lignin BO yield was closely related to FA/feedstock mass ratio since the contour lines were nearly perpendicular to the x-axis. This could be attributed to the positive role that FA plays in lignin depolymerization, as previously discussed. The yield of BO generated from de-alkaline lignin dramatically decreased with increasing temperature when the FA/feedstock mass ratio was at its lowest setting (0.5). However, the de-alkaline lignin BO yield showed no remarkable changes with increasing temperature when FA/feedstock mass ratio (or FA loading) was at its higher setting (>1), indicating that the effect of temperature might be masked by the outstanding effect of FA.

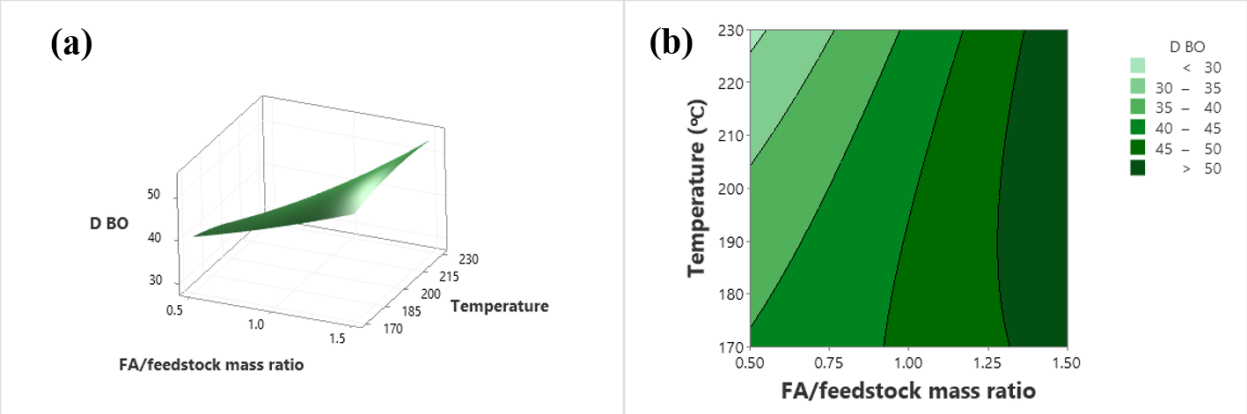

Figure 4.4 The response surface plot (a) and contour plot (b) for de-alkaline lignin BO yield as a function of FA/feedstock mass ratio and temperature

The interaction effect between "FA/feedstock mass ratio" and "Temperature" in response to the yield of PM derived from de-alkaline lignin is presented in Fig. 4.5. It can be noted that the increasing FA/feedstock mass ratio from 0.5 to 1.5 gave rise to a remarkable increase in de-alkaline PM yield. Moreover, the positive effect of FA seemed to become more outstanding when the temperature was high (200-230℃). The optimal temperature resulting in the highest yield of de-alkaline lignin PM was relatively moderate (around 190℃) when the FA/feedstock mass ratio was at its lowest setting (0.5). However, as the FA/feedstock mass ratio was raised up to a higher level (1.5), the most suitable temperature for the production of de-alkaline lignin PM was approximately 210℃. This observation reiterated that the amount of FA required for sufficient lignin depolymerization (or PM production) was probably correlated with the temperature due to the competition between depolymerization and repolymerization reactions.

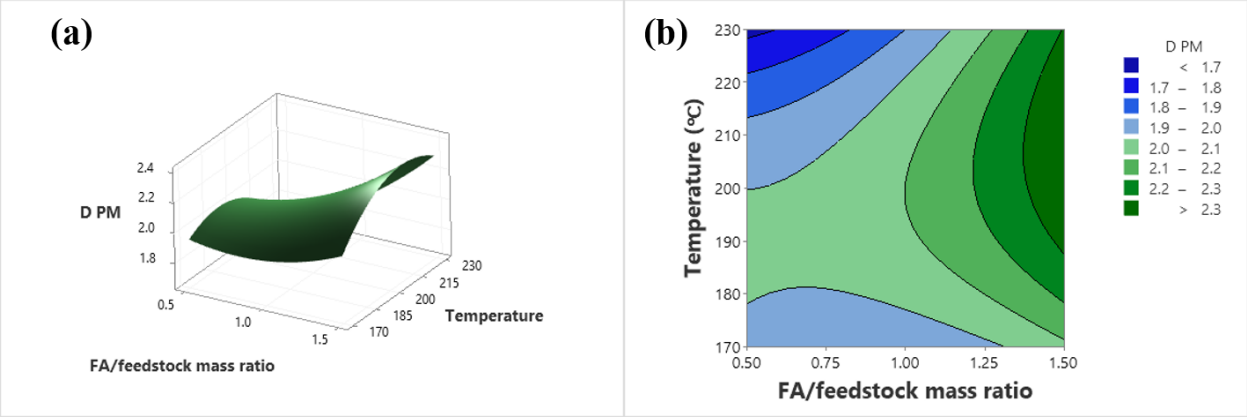

Figure 4.5 The response surface plot (a) and contour plot (b) for de-alkaline lignin PM yield as a function of FA/feedstock mass ratio and temperature

4.4. Conclusions

In this chapter, a general 2^k factorial design with replicating center points was applied to evaluate the curved relationship between factors of interest (feedstock concentration, FA/feedstock mass ratio, temperature, and retention time) and the responses (alkaline lignin BO/PM yield, and de-alkaline lignin BO/PM yield) in MW-assisted lignin depolymerization. Based on the statistical analysis, at least one factor of interest has a curved relationship with the response, indicating that a CCD of RSM is suitable to further investigate the effects of factors on the responses in this study.

The CCD provided a preliminary understanding about the effects of process variables on the yields of BO and PM obtained in the MW-assisted depolymerization of alkaline lignin and de-alkaline lignin in the presence of FA. Among four factors of interest, FA/feedstock mass ratio was identified as the most dominant factor affected both BO yield and PM yield. The positive effect of

FA could be explained by the fact that FA did not merely serve as a hydrogen donor but also react with lignin through a formylation-elimination-hydrogenolysis mechanism, leading to the depolymerization of lignin biopolymer and stabilization of lignin-derived fragments under the synergistic effect with ethanol solvent.

A few FA-involved 2-way interaction effects were also significant. When alkaline lignin BO yield was selected as the response, the interaction between “Feedstock concentration” and “FA/feedstock mass ratio” suggested that the amount of FA required for lignin depolymerization might seemed correlate with feedstock concentration due to different concentration of FA in the solvent system. The beneficial influence of FA became more remarkable when the feedstock concentration was high, which means that the initial FA concentration in solvent system was high. Regarding de-alkaline lignin BO yield, the interaction between “FA/feedstock mass ratio” and “Temperature”, it could be elucidated that the negative impact of increasing temperature on de-alkaline lignin BO yield was gradually diminished as FA/feedstock mass ratio was elevated. In terms of the significant interaction between “FA/feedstock mass ratio” and “Temperature” on PM yield derived from alkaline and de-alkaline lignin, it is speculated that the promoting effect of FA on stabilizing the reactive lignin-derived intermediates intensely compete with the enhanced repolymerization reactions induced by excessively increasing temperature within the selected experimental range.

Chapter 5: Optimization of Microwave-assisted Lignin Depolymerization for Bio-oil and Phenolic Monomer Production

Chapter 4 has identified the most influential process variables on product yields in lignin depolymerization. This chapter aims to develop regression models and to further find out the optimal experimental conditions that maximize the yield of BO and PM generated from either alkaline lignin or de-alkaline lignin. In continuation to the previous chapter, four process variables that were taken into considerations include feedstock concentration, FA/feedstock mass ratio, temperature, and retention time. Lignin-derived products were characterized and presented in this chapter.

5.1. Regression Model Development

The experimental data of CCD presented in the Chapter 4 was analyzed using Minitab software and fitted to the following second-order polynomial model:

$$y = \beta_0 + \sum_{i=1}^{k} \beta_i x_i + \sum_{i=1}^{k} \beta_{ii} x_i^2 + \sum_{i=1} \sum_{i<j} \beta_{ij} x_i x_j$$

Where y is the response, x_i and x_j are the coded independent variables, β_0 is the intercept coefficient, β_i is the linear coefficient, β_{ii} is the quadratic (or second-order) coefficient, β_{ij} is the interaction coefficient. The validity of normal distribution assumption and constant variance assumption on the error terms was verified by constructing a normal probability plot (NPP) of the residues, and a residues against the fitted values plot was created as described in (Montgomery, 2017).

The full quadratic regression models were suggested by Minitab 19.0 software for the four responses, and the following regression models were developed (significant model terms are shown in bold):

The alkaline lignin derived BO yield regression model for the coded level is expressed in the below equation:

$Y_{\text{alkaline BO}} = 275.5 - 17.09\mathbf{X_1} - 78.5\mathbf{X_2} - 1.119X_3 + 0.305X_4 + 0.3333\mathbf{X_1^2} + 13.51X_2^2 + 0.00096X_3^2 - 0.00173X_4^2 + 1.669\mathbf{X_1X_2} + 0.03163\mathbf{X_1X_3} - 0.00096X_1X_4 + 0.2380\mathbf{X_2X_3} + 0.0987\mathbf{X_2X_4} - 0.000246X_3X_4$

The de-alkaline lignin derived BO yield regression model for the coded level is described in the below equation:

$Y_{\text{de-alkaline BO}} = 75.2 - 0.90X_1 - 48.6\mathbf{X_2} + 0.102\mathbf{X_3} - 0.229X_4 - 0.1014X_1^2 + 2.10X_2^2 - 0.00136X_3^2 + 0.00132X_4^2 + 1.047\mathbf{X_1X_2} + 0.01304\mathbf{X_1X_3} + 0.00285X_1X_4 + 0.2115\mathbf{X_2X_3} + 0.0479X_2X_4 - 0.000508X_3X_4$

The alkaline lignin derived PM yield regression model for the coded level is shown in the below equation:

$Y_{\text{alkaline PM}} = 19.31 - 0.385X_1 - 2.74X_2 - 0.1359X_3 - 0.0055X_4 + 0.01415\mathbf{X_1^2} - 0.385X_2^2 + 0.000279X_3^2 - 0.000078X_4^2 + 0.0203X_1X_2 - 0.000424X_1X_3 + 0.000418X_1X_4 + 0.01839\mathbf{X_2X_3} - 0.00422X_2X_4 + 0.000091X_3X_4$

The de-alkaline lignin derived PM yield regression model for the coded level is described in the below equation:

$Y_{\text{de-alkaline PM}} = -4.01 + 0.095X_1 - 2.707\mathbf{X_2} + 0.0760X_3 - 0.0192X_4 - 0.00474X_1^2 + 0.352X_2^2 - 0.000210\mathbf{X_3^2} + 0.000092X_4^2 + 0.0347\mathbf{X_1X_2} + 0.000002X_1X_3 + 0.000048X_1X_4 + 0.00844\mathbf{X_2X_3} + 0.00174X_2X_4 - 0.000008X_3X_4$

Where X_1 is the feedstock concentration (wt.%); X_2 is the FA to feedstock mass ratio; X_3 is temperature (°C); X_4 is retention time (min).

Table 5.1 shows a summary of four regression models, which help to determine whether the regression models are well-fitted. Regression coefficient R-square (R^2) refers to the percentage of variation in the response that can be explained by the model, which is always between 0% and 100%. The higher the R^2 value, the better the model fits the experimental data. Adjusted R-square (Adj R^2) is another measurement of how well the model fits the data, which adjusts R^2 for the number of predictors in the model relative to the number of observations. In our work, the Adj R^2 values for alkaline lignin BO yield (94.05%) and de-alkaline lignin BO yield (90.59%) demonstrated that both regression models were well fitted. Fig. 5.1 further graphically illustrated how well the actual values of the responses fitted into their corresponding predicted values, which fell on the fitted regression line. However, the Adj R^2 values for alkaline lignin PM yield (65.01%) and de-alkaline lignin PM yield (67.25%) are less satisfactory, as graphically depicted in Fig. 5.2. This was likely due to the various types of systematic or random errors introduced during the experimental processes and product characterization process (e.g. solvent evaporation for BO recovery and GCMS analysis for the determination of PM yield).

Table 5.1 The fit summary of regression models

Response	Model F-value	Model p-value	R-square	Adj R-square
Alkaline BO yield	34.88	0.00	96.83%	94.05%
De-alkaline BO yield	21.63	0.00	94.98%	90.59%
Alkaline PM yield	4.98	0.00	81.34%	65.01%
De-alkaline PM yield	5.40	0.00	82.53%	67.25%

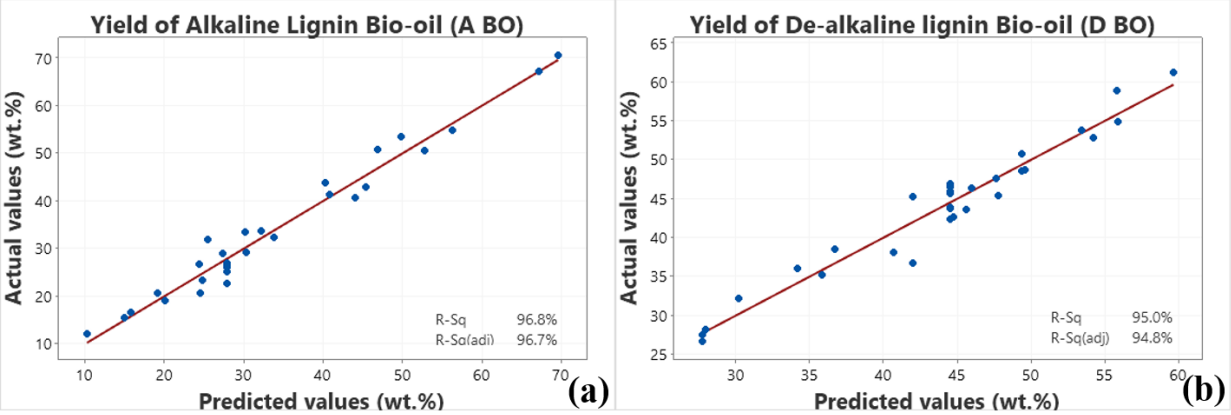

Figure 5.1 Actual vs. predicted values of alkaline lignin BO yield (a) and de-alkaline lignin BO yield (b)

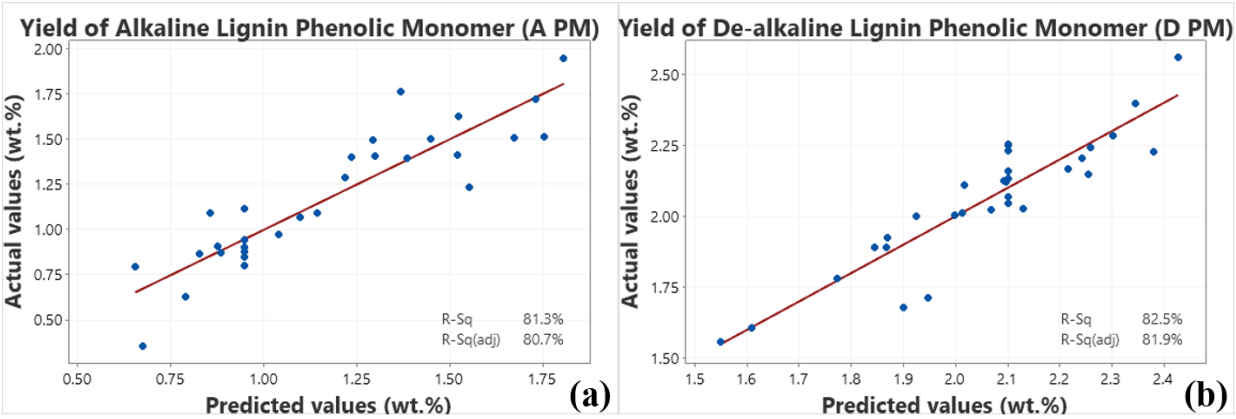

Figure 5.2 Actual vs. predicted values of alkaline lignin PM yield (a) and de-alkaline lignin PM yield (b)

5.2. Optimal Reaction Conditions

In order to maximize the yield of BO and PM derived from alkaline and de-alkaline lignin, the optimal reaction conditions were obtained by the response optimizer and summarized in Table 5.2. The optimization plots for alkaline and de-alkaline lignin were shown in Fig. 5.3 and Fig. 5.4, respectively. The importance levels of two responses (BO yield and PM yield) were set as the default value of 1, indicating that two responses are equally important. The optimal reaction

conditions for alkaline lignin depolymerization are: feedstock concentration of 20%, FA/feedstock mass ratio of 1.5, temperature of 230℃, and retention time of 110.91min. The predicted yields of BO and PM derived from alkaline lignin were 71.25% and 1.73% respectively, with a composite desirability of 94.66%. The optimal reaction conditions for de-alkaline lignin depolymerization are: feedstock concentration of 17.27, FA/feedstock mass ratio of 1.5, temperature of 208.79℃, and retention time of. 140min. The predicted yields of BO and PM derived from de-alkaline lignin were 59.40% and 2.59% respectively, with a composite desirability of 93.35%.

Table 5.2 Optimum operating conditions

	Optimum operating conditions				Predicted product yield	
Lignin type	Conc (%)	FA ratio	Temp (℃)	Time (min)	BO yield (%)	PM yield (%)
Alkaline	20.00	1.5	230.00	110.91	71.25	1.73
De-alkaline	17.27	1.5	208.79	140.00	59.40	2.59

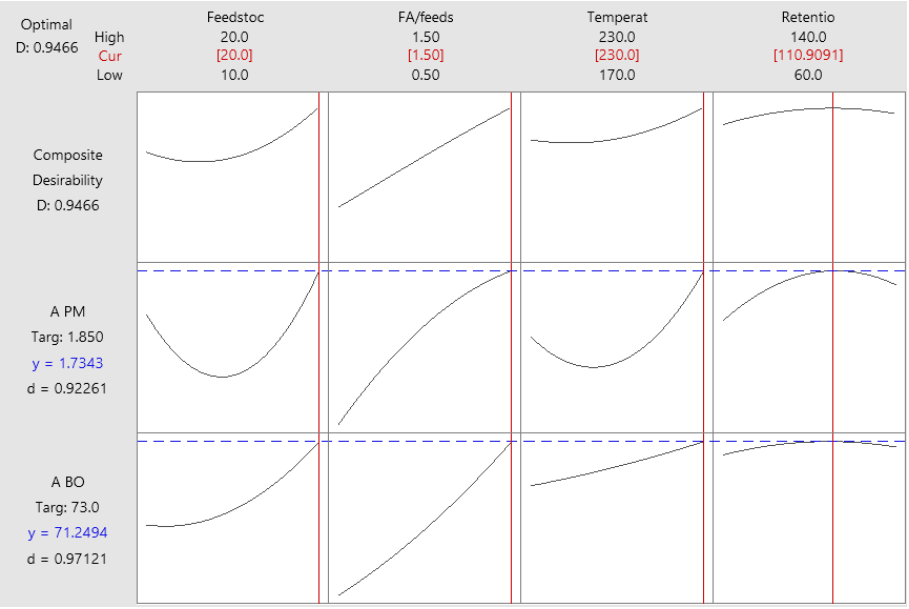

Figure 5.3 Optimization plot of alkaline lignin

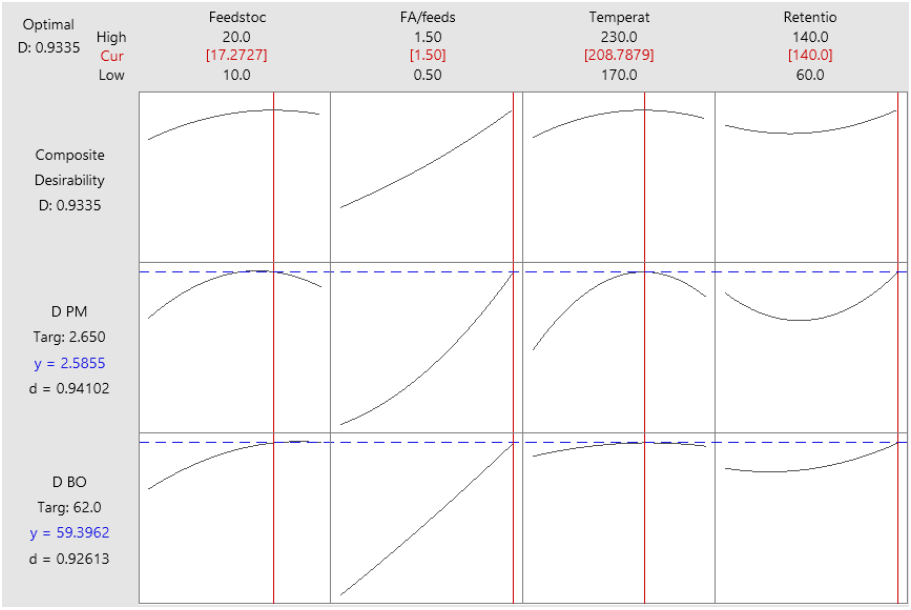

Figure 5.4 Optimization plot of de-alkaline lignin

5.3. Product Characterization

Fig. 5.5 presents the distribution of PM in alkaline and de-alkaline BO. The monomeric phenolic compounds were categorized into three groups, including phenol (H) type, guaiacol (G) type and syringol (S) type that contain zero, one, and two methoxyl groups (O-CH_3) respectively. It can be noted that cresol and guaiacol are dominant monomeric phenolic compounds in alkaline BO, accounting for 23.70% and 21.35% of the total PM respectively. When it comes to de-alkaline lignin, vanillin is identified as the most dominant monomeric phenolic compound in BO, which makes up approximately one third (32.72%) of the total PM derived from MW-assisted depolymerization. Followed by vanillin, 1-(4-hydroxy-3-methoxyphenyl)-2-Propanone and 2-methoxy phenol (guaiacol) are also relatively abundant monomers, taking up 12.01% and 12.91% of the total PM individually. Other types of GC-detectable PM in the BO derived from two lignin feedstocks are summarized in Table S.1 and Table S.2 in Appendix. Overall, G type compounds accounted for 97.70% of the total PM derived from de-alkaline lignin while took up 73.43% of the total GC-detectable PM generated from alkaline lignin. The abundance of G type compounds in de-alkaline lignin BO could be attributed to the fact that the ^{13}C nuclear magnetic resonance (NMR) spectrum of de-alkaline lignin exhibited a pronounced intensity of methoxyl groups in respect to alkaline lignin, as reported by Zhou et al. (2019).

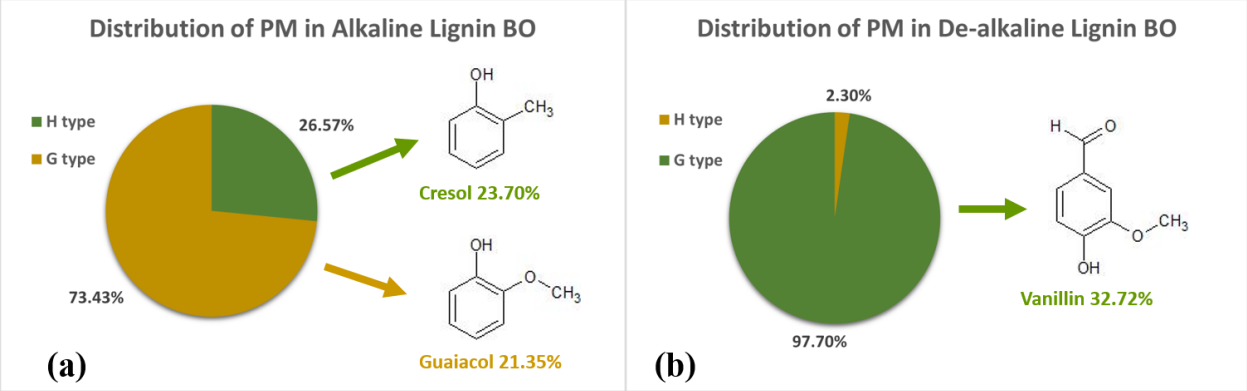

Figure 5.5 Distribution of PM in BO from alkaline (a) and de-alkaline (b) lignin

According to the ICP mineral content analysis on the BO provided by SGS Agri-Food Laboratories, it can be revealed that the obtained BO derived from direct evaporation (DE) of reaction solvent contained significant amount of sodium (17.11%). This observation could be explained by the product preparation information provided by the supplier (TCI company) that both types of lignin feedstock were prepared from sodium lignosulfonate (LS) yielded from the sulfite process, wherein sodium sulfite (Na_2SO_3) is typically used as the reagent. Based on our calculations on mass transfer, 80wt.% of sodium in the lignin feedstock was transferred into BO.

5.4. Conclusions

In this chapter, regression models were developed for four responses, including alkaline lignin BO yield, de-alkaline lignin BO yield, alkaline lignin PM yield, and de-alkaline lignin PM yield. The regression models for alkaline lignin BO yield and de-alkaline lignin BO yield are well fitted with the experimental data, with high adj R^2 values of over 90%. However, the regression models for alkaline lignin PM yield and de-alkaline lignin PM yield are less satisfactory, with relatively low adj R^2 values (below 70%). This could be attributed to the various types of systematic or random errors introduced during the experimental processes and product characterization process.

Within the experimental design range, the optimal experimental conditions for MW-assisted alkaline and de-alkaline lignin depolymerization were obtained using a response optimizer, assuming that BO and PM yields for each feedstock were equally important. The optimal reaction conditions for alkaline lignin depolymerization are: feedstock concentration of 20%, FA/feedstock mass ratio of 1.5, temperature of 230°C, and retention time of 110.91min. The optimal reaction conditions for de-alkaline lignin depolymerization are: feedstock concentration of 17.27,

FA/feedstock mass ratio of 1.5, temperature of 208.79℃, and retention time of 140min. The yield of BO generated from alkaline and de-alkaline lignin were optimized to 71.25% and 59.40% respectively, while PM yields derived from two types of lignin feedstocks were optimized to 1.73% and 2.59%.

In terms of product characterization with the assistance of GCMS, cresol and guaiacol are dominant monomeric phenolic compounds in alkaline BO while vanillin is identified as the most dominant monomeric phenolic compound in de-alkaline lignin BO. According to the ICP metal analysis, 80wt.% of sodium in alkaline lignin feedstock was transferred into BO. This finding suggested that the obtained BO contained a large amount of impurities which lowed the quality of lignin-derived BO.

Chapter 6: Investigation of Downstream Processing Method on Products Recovery from Microwave-assisted Lignin Depolymerization

In the previous chapters, BO derived from lignin was obtained by a direct evaporation (DE) method to remove reaction solvent through nitrogen entrainment. However, based on our observations, the quality of the obtained BO was poor and it could not be completely dissolved in THF before being injected into GCMS, even with the assistance of ultrasound as shown in Fig. 6.1. In addition, ICP metal analysis found that about 80 wt.% of sodium in lignin feedstock was left in BO, indicating that the obtained BO might contain considerable amounts of impurities. These observations suggested there was a need to develop a proper downstream processing method to remove these impurities and to recover bio-oil with better quality.

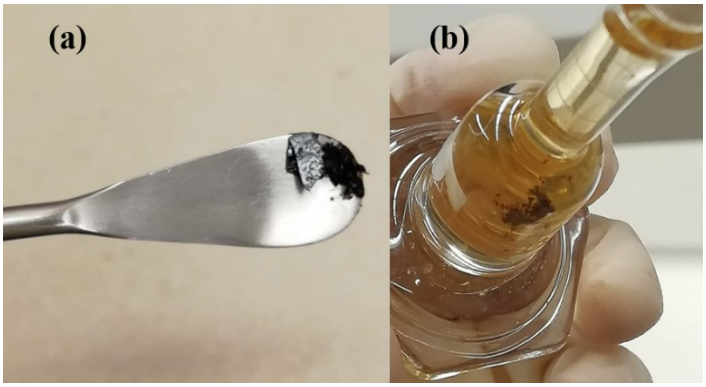

Figure 6.1 Low quality BO with a brittle solid texture (a) and the observed insoluble precipitation in THF solution (b)

In the past few years, depolymerization of isolated lignin has become an extensively investigated research topic, resulting in a large number of depolymerization studies. Nevertheless, little research has been conducted to elucidate the impacts of downstream processing on the yield and physicochemical properties of products derived from lignin depolymerization. In addition, the downstream processing procedures reported in the currently available literature vary significantly with the type of lignin and the selected reaction solvent systems (e.g. single aqueous/organic solvent system and binary solvent system). As summarized in Table 6.1, the different downstream processing methods often does not allow a straightforward comparison of lignin depolymerization studies, even though the same solvent system (ethanol/FA cosolvent) was selected as the reaction media. Moreover, it could be impracticable to directly apply a downstream processing method that had been validated in the literature, due to different sources of variability during lignin depolymerization experiments (e.g. different lignin feedstocks, different reaction conditions and

different scales of reactors). For example, depolymerization of Eucalyptus lignin and Alcell® lignin in ethanol/FA cosolvent resulted in two immiscible layers including a dark-color BO layer on top and a clear layer on the bottom of product mixture, as reported by Ghoreishi et al. (2019a, 2019b) and Kloekhorst et al. (2015). These experimental phenomena were completely different from our hands-on experience that a single-phase product mixture was obtained after the reaction. On the other hand, various pH adjustment prior to product recovery in the currently available literature aroused our interests. As reported by Dong et al. (2014), the pH level of liquid product derived from lignin depolymerization was adjusted to 6, followed by ethyl acetate-assisted extraction of BO. Milovanović et al. (2016) proposed a downstream separation procedure for BO recovery, in which the pH level of liquid product was adjusted back and forth (from acid range to alkaline range and back to acid range) prior to BO extraction, for no specified reasons.

This chapter therefore aims to develop an "in-house" downstream processing protocol for lignin feedstocks of interest under the experimental conditions in this study. Furthermore, the impacts of downstream processing method and pH adjustment on the yields of BO and PM, as well as the physicochemical properties of BO, were investigated.

Table 6.1 A summary of downstream processing methods applied in lignin depolymerization experiments when ethanol/FA cosolvent is the reaction media

Feedstock	Reaction solvent	Description of downstream processing method	Reference
Eucalyptus lignin	Ethanol/FA cosolvent	After the reaction was completed, the liquid phase consisted of two immiscible layers: a dark-brown BO phase and a small clear ethanol/water phase. The BO phase was extracted using a solution of ethyl acetate : THF (90:10). The extracted BO phase was dried over Na_2SO_4 and evaporated using a rotary evaporator at 40℃ and 175mbar to obtain BO.	(Ghoreishi et al., 2019b, 2019a)
Concentrated acid hydrolysis lignin	Ethanol/FA cosolvent	The liquid/solid mixture was collected by washing the reactor with acetone and separated by vacuum filtration. The BO was obtained by evaporating the at 70℃ at reduced pressure using a rotary evaporator, followed by drying at 105℃ for 3h to remove the moisture.	(Kristianto et al., 2017)
Alcell® lignin	Ethanol/FA cosolvent	The liquid/solid mixture was separated by filtration. The filtrate typically consists of two immiscible layers: a clear colorless layer on the bottom and a dark black oil phase on top. The oil phase was heated to 300K (27℃) under vacuum to remove the volatiles and the solvent. The remaining oil phase was designated as lignin BO.	(Kloekhorst et al., 2015)
Organosolv switchgrass lignin	Ethanol/FA cosolvent	The product mixture was filtered remove any solid residues. The filtrate was directly used for GC-MS and GPC analyses without an evaporation process to obtain BO yield.	(Xu et al., 2012)
Wheat straw alkali lignin	Ethanol/FA cosolvent	After the reaction, water and sodium hydroxide was added into the reaction mixture to adjust pH to 2. The mixture was filtered to separate solid residue from the liquid phase. Both the filtrate and the solid residue were extracted with ethyl acetate to obtain a combined organic phase. The lignin BO was obtained by the evaporation of ethyl acetate in organic phase.	(Ouyang et al., 2015)
Concentrated sulfuric acid hydrolysis lignin	Ethanol/FA cosolvent	The liquid and solid products were washed with acetone and separated using vacuum filtration. The filtrate was evaporated using a rotary evaporator at 50℃ and reduced pressure (to remove acetone). The obtained liquid was dried in a vacuum oven at 70℃ for 24h (for ethanol removal) to obtain BO.	(Riaz et al., 2016)
Lignin produced from oakwood and pinewood	Ethanol/FA cosolvent	The reaction mixture was washed with acetone. The liquid and solid products were separated by filtration. The liquid product was evaporated at 50℃ and 0.02MPa using a rotary evaporator (to remove acetone). After the evaporation process, the BO was further dried in a vacuum oven at 60℃ for 6h to remove the residual ethanol.	(Park et al., 2018)
Concentrated sulfuric acid hydrolysis lignin	Ethanol/FA cosolvent	The liquid and solid products in the reactor were collected by acetone washing and were separated by filtration. The filtrate containing BO, unreacted ethanol and acetone was rotary-evaporated at 60℃ and 0.08MPa for 0.5h. After evaporation, the recovered BO was further dried in an oven at 80℃ for 72h to remove the remaining solvents.	(Hidajat et al., 2018)
Rice straw lignin	Ethanol/FA cosolvent	The product mixture was extracted with a solution of ethyl acetate : THF (90:10) and filtered to separate solid phase and liquid phase. The dark-brown organic liquid phase was dried over anhydrous Na_2SO_4 and concentrated at a reduced pressure (160mbar) at 40℃ to obtain BO.	(Oregui-Bengoechea et al., 2018)

6.1. An "In-house" Downstream Recovery Protocol

Two lignin feedstocks, alkaline and de-alkaline lignin, were depolymerized under the reaction conditions with a temperature of 230℃, a retention time of 140min, a feedstock concentration of 8% and a FA/DAF lignin mass ratio of 2. The resulting bio-oil was recovered by a "in-house" developed ethyl acetate-water extraction method. Fig. 6.2 shows a schematic representation of this downstream recovery protocol. Three different pH levels, including 1 ,7, and 13, were applied to investigate the impacts of downstream pH adjustment on the extraction efficiency.

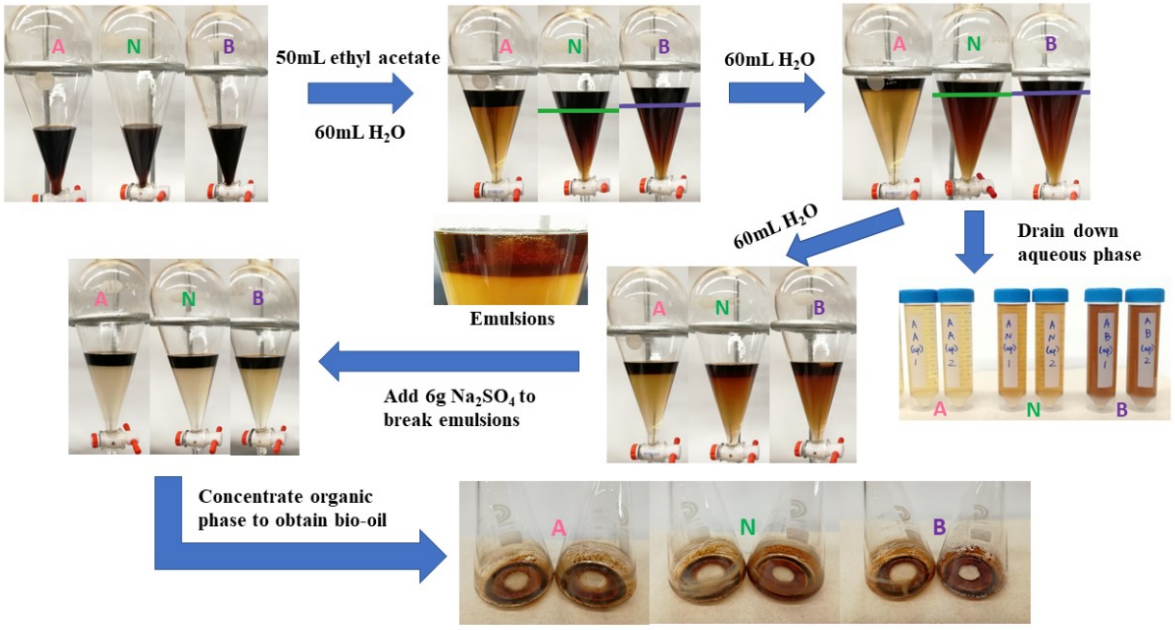

Notes: "A", "N" and "B" denote "acidic condition", "neutral condition" and "basic condition" respectively

Figure 6.2 Schematic representation of in-house downstream recovery protocol

The influences of downstream pH adjustment on BO yield and PM yield were investigated and results are presented in Fig. 6.3 and Fig. 6.4.

Fig. 6.3 shows that the yields of BO and PM recovered from liquid-liquid extraction (LLE) were closely associated with the downstream pH level. As the pH value decreased from 13 to 1, the yield of BO derived from alkaline lignin notably increased from 12.53% to 21.47%. Similar trend was also observed for the yield of BO from de-alkaline lignin. With the increase in acidity of extraction environment, the yield of de-alkaline lignin BO gradually rose from 14.20% to 25.07%. When it comes to the effects of pH adjustment on PM yield, a decline in pH contributed to a remarkable increase in alkaline lignin PM yield from 2.94% to 4.35%. The yield of de-alkaline

lignin PM yield also exhibited a rising trend, from 2.65% to 4.20%. Based on these observations, it seemed that the extraction efficiency of lignin-derived products was pH-sensitive, and an acidic condition is more favorable than a basic condition for the extraction yields of BO and PM. This could be explained by the fact that the pH level of solution affects in ionization of solutes and further influences the affinity between the solutions and the solutes as reported by Fu et al. (2007). Under alkaline conditions, the hydroxyl groups in phenolic compounds are dissociated to hydrogen ions and their corresponding anions (e.g. phenolate anion), which are more soluble in water than in the organic solvent (Abbassian et al., 2014; Wang et al., 2013). Based on this possible reason, the extraction efficiency decreased considerably when pH was adjusted to a higher level. However, the effects of pH on the extraction efficiency is complex and are strongly dependent on the solvent used as well as the physicochemical properties of desired products. In our study, the extraction system was even more complex as three types of solvents, namely water, ethanol, ethyl acetate were involved in the liquid-liquid extraction (LLE) of BO and PM, making the partition of phenolic compounds between the two phases become more unpredictable. Another possible reason for the pH-associated variation of extraction efficiency is that phenolic compounds were largely unstable and could be more susceptible to oxidative degradation when exposed to alkaline conditions, as reported in the literature (Chethan & Malleshi, 2007; Friedman & Jürgens, 2000).

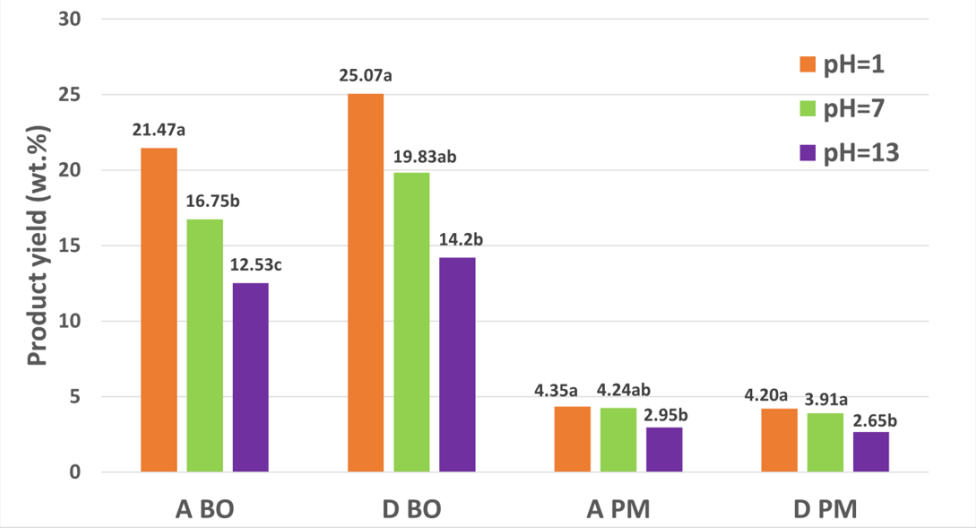

Figure 6.3 Effect of downstream pH level on BO and PM yield

Notes: A BO=alkaline lignin BO yield; D BO=de-alkaline lignin BO yield; A PM=alkaline lignin PM yield; D PM=de-alkaline lignin PM yield

As seen in Fig. 6.4, the type of lignin feedstocks did not have a significant effect on either BO yield or PM yield derived from MW-assisted depolymerization, regardless of the pH level applied for the downstream recovery.

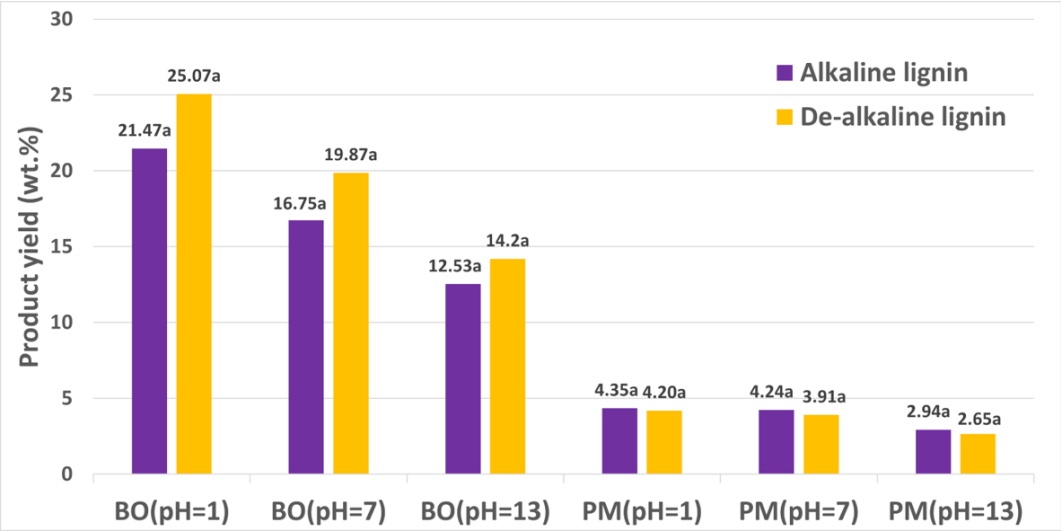

Figure 6.4 Effect of lignin feedstocks on BO and PM yield at different pH levels

6.2. Comparison between Newly Developed Liquid-Liquid Extraction Method and Direct Evaporation Method in Bio-oil Recovery

Based on visual examination, the newly developed liquid-liquid extraction (LLE) downstream processing protocol resulted in higher quality BO with good liquidity instead of solid texture. For comparison purposes, two types of lignin feedstocks were also depolymerized under the same conditions specified in section 6.1 and the resulting BO was recovered by direct evaporation (DE) of reaction solvent method. Thus the effects of downstream processing methods on product yield were investigated and results are depicted in Fig. 6.5. As presented in Fig. 6.5, the yield of alkaline lignin BO dramatically decreased from 42.64% to 21.47% when LLE was applied. In terms of de-alkaline lignin BO yield, a sharp reduction from 48.38% to 25.07% was also observed with the alteration of downstream processing method. However, only negligible changes (not statistically significant) in PM yield can be detected when LLE under acidic conditions was selected as the downstream processing method, regardless of the type of lignin feedstocks. This observation suggests that LLE under acidic conditions might be a good method to remove impurities from the organic phase containing BO.

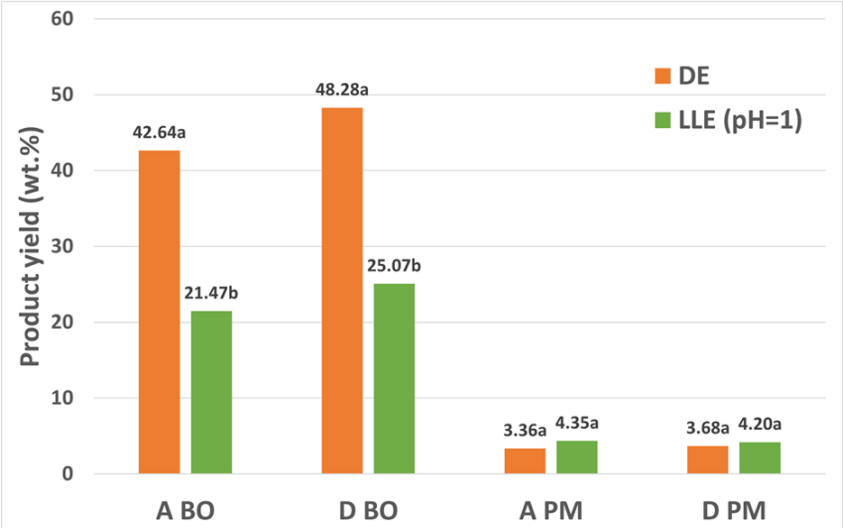

Figure 6.5 Effect of downstream processing method on product yield

Notes: DE= direct evaporation of reaction solvent; LLE = liquid-liquid extraction

Table 6.2 presents the average molecular mass (M_n and M_w) of the BO derived from two different downstream processing methods. The results indicates that the relative molecular mass and distributions of the obtained BO products were similar, where the M_n, M_w and PDI were in the range of 536 to 583g/mol, 801 to 917g/mol, and 1.49 to 1.57, respectively. The weight average molecular mass (M_w) of lignin-derived BO was comparable to the result reported by Park et al. (2016), in which BO with a Mw ranging from 969 to 1057g/mol was obtained from non-catalyzed lignin depolymerization in ethanol/FA cosolvent operated at 350°C for 40min. Based on the one-way ANOVA using Fisher LSD test, alkaline lignin BO has a higher average molecular mass than de-alkaline lignin BO, regardless of the downstream processing method. This observation suggested that the degree of depolymerization of de-alkaline lignin might be higher than that of alkaline lignin under the same reaction conditions, resulting in a lower average molecular mass of phenolic BO. On the other hand, downstream processing method did not have a significant effect on the average molecular mass of phenolic BO, regardless of the type of lignin feedstock.

Table 6.2 Average molecular mass of BO obtained from MW-assisted lignin depolymerization

Sample	M_n (g/mol)	M_w (g/mol)	PDI
A BO derived from DE	570 A	893 A	1.57 A
D BO derived from DE	536 B	801 B	1.49 B
A BO derived from LLE	583 A	917 A	1.57 A
D BO derived from LLE	551 B	828 B	1.50 B

Note: A BO=alkaline lignin bio-oil; D BO=de-alkaline lignin bio-oil; DE=direct evaporation of reaction solvent, LLE=liquid-liquid extraction

The chromatograms presented in Fig 6.6 and Fig. 6.7 show that the composition of the GC-detectable part of the BO is very similar when two different downstream processing methods were applied (DE to remove organic solvent vs. LLE using ethyl acetate and water). It is observed that guaiacol and vanillin were the most abundant phenolic compounds in bio-oil derived from alkaline and de-alkaline lignin respectively, under the specific reaction conditions applied in this study.

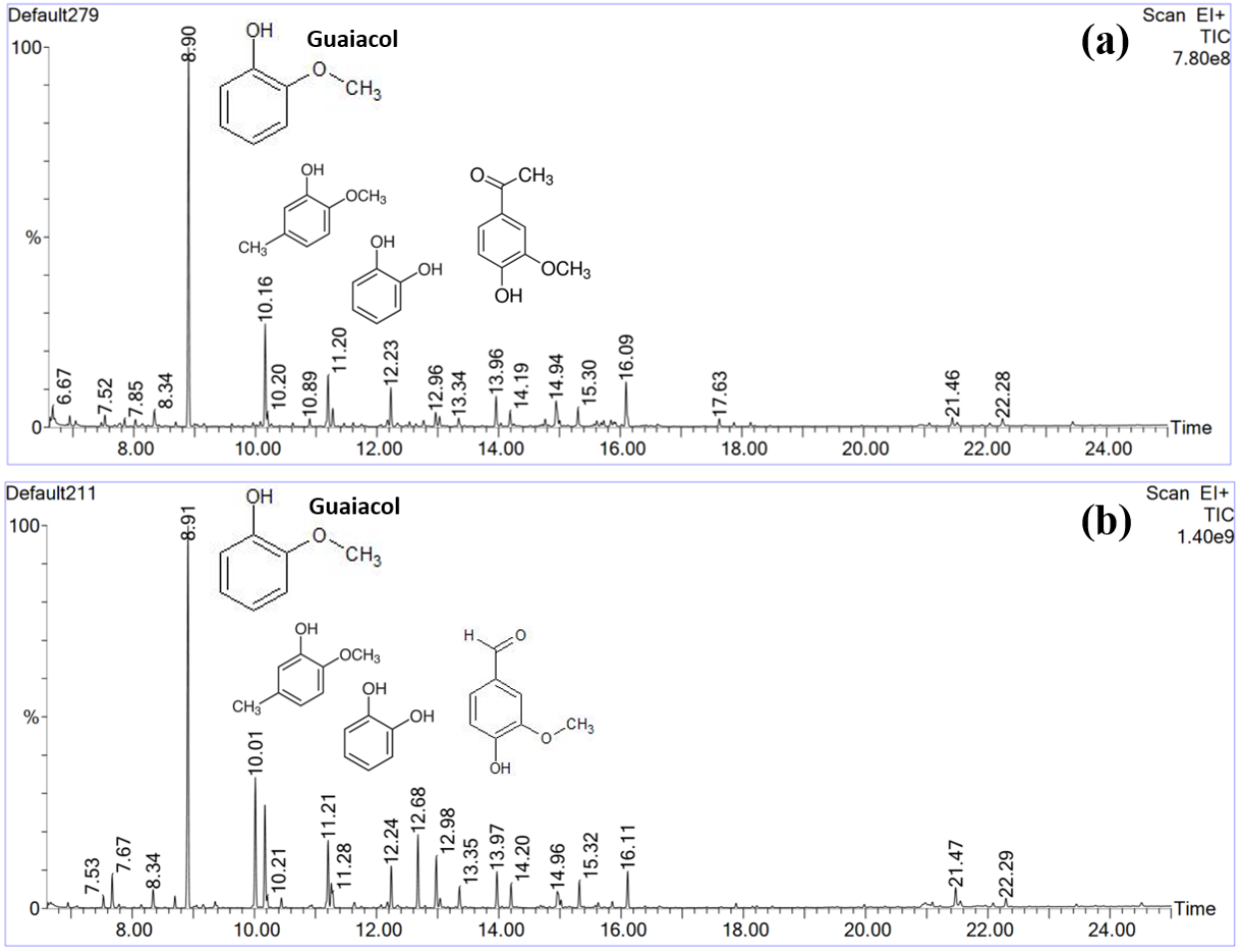

Figure 6.6 GC-MS chromatograms of alkaline lignin BO from DE (a) and LLE (b)

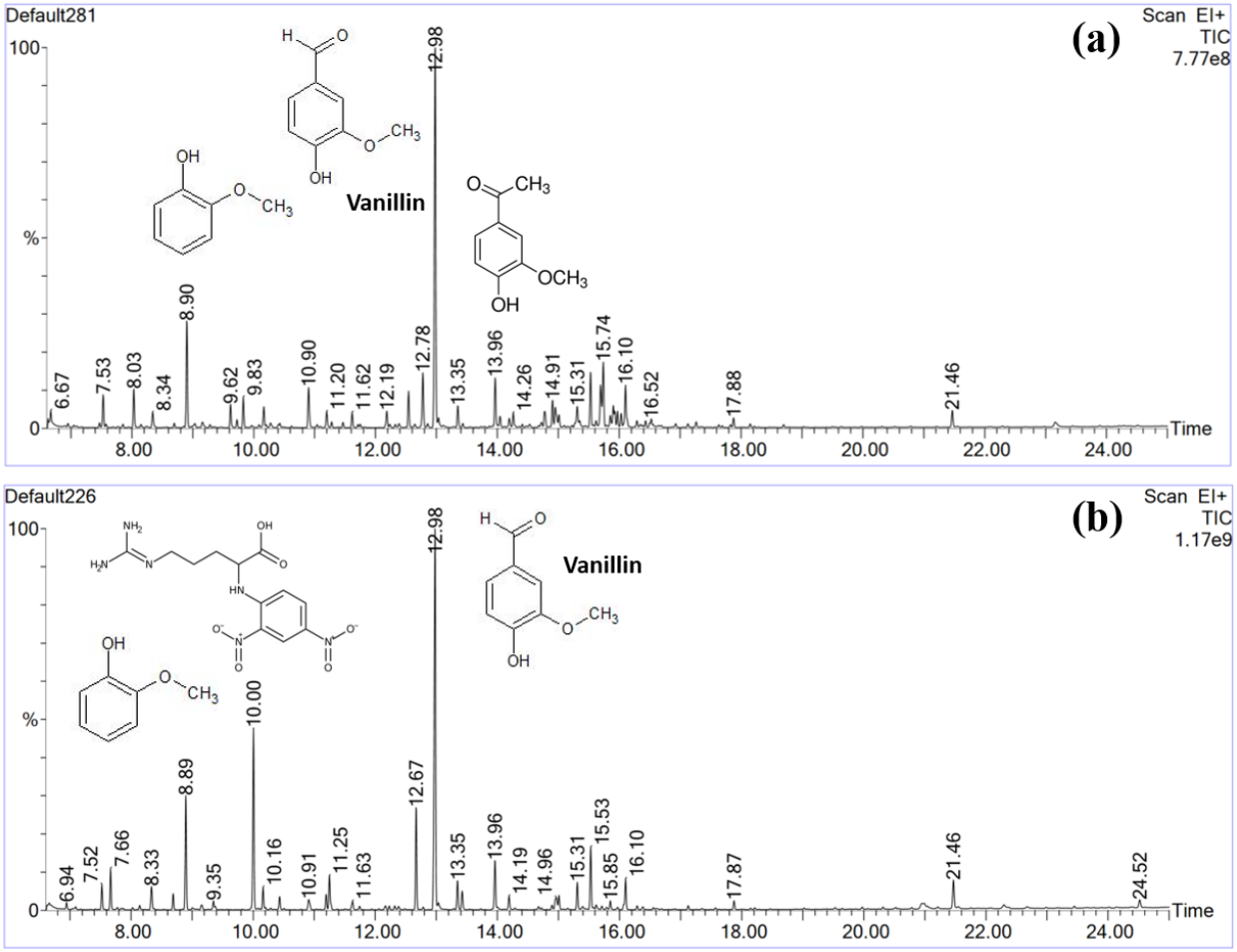

Figure 6.7 GC-MS chromatograms of de-alkaline lignin BO derived DE (a) and LLE (b)

6.3. Conclusions

In this chapter, an "in-house" downstream processing protocol was developed, in which ethyl acetate and distilled water were used to extract PM-rich BO from lignin depolymerization.

It is found that two-phase LLE using both water and ethyl acetate as extractants is an effective way to recover BO derived from MW-assisted lignin depolymerization. Adjusting pH value of liquid organic phase before extraction greatly impacted the yields of BO and PM. The extraction efficiency of lignin-derived products is closely associated with the pH level in downstream extraction. The experimental results indicated the acidic condition favored the recovery of BO and PM than the neutral or basic condition. This was due to the altered affinity between the solutes and the extraction solvents, being induced by ionization of solutes (phenolic compounds) when exposed to different pH levels. The study on the influences of lignin feedstocks has shown that the type of lignin feedstocks did not have a significant effect on either BO yield or

PM yield, regardless of the pH level applied in the downstream recovery process. The experimental results also verified that regarding the quality of bio-oil, the newly developed ethyl acetate/water-based LLE method performed much better than the nitrogen purging-based DE method. Dramatic decreases in BO yield were observed when LLE was used to recover BO, while only negligible changes in PM yield was detected for both alkaline lignin and de-alkaline lignin. This observation suggested that LLE under acidic condition could be an efficient method to remove impurities (e.g. inorganic metal salts) in liquid organic phase resulting from lignin depolymerization. In terms of the properties of BO, de-alkaline lignin BO had a lower average molecular mass than alkaline lignin BO, regardless of the downstream processing method employed.

Chapter 7: Microwave-assisted Lignin Depolymerization in Aqueous Solvent System

In Chapter 4, 5 and 6, MW-assisted lignin depolymerization involving the use of FA and ethanol meets the sustainability and renewable criteria, since all the reactants can be generated from renewable resources. FA is one of the main side-products derived from cellulose and hemicellulose hydrolysis, as well as sugar conversion processes (Chen et al., 2020). Moreover, cellulosic ethanol, which can be produced from waste biomass (e.g. wheat straw, sugarcane bagasse, and corn stover) has become a highly desirable substitute for fossil fuel (Li & Takkellapati, 2018). However, this method still involves handling organic solvent, ethanol which is undesirable from green chemistry perspective. It would be encouraging to use green, low cost and largely available water as an alternative reaction medium. Another consideration is that most studies reported in the literature have been focusing on catalytic lignin depolymerization in either ethanol or water. There are not much research presenting a comparison of the solvent effect between ethanol and water. Therefore, this chapter aims to explore a MW-assisted lignin depolymerization in aqueous solvent system and to compare it to ethanolic solvent system.

As the main focus of this study is to compare the performance of aqueous and ethanolic solvent systems as the reaction medium for MW-assisted lignin depolymerization in the presence of FA, the depolymerization condition used in Chapter 6 was applied in this chapter to ensure a straightforward comparison between two types of green solvents.

7.1. Effect of Reaction Solvent on Product Yields

Alkaline and de-alkaline lignin were depolymerized in water and ethanol respectively at a temperature of 230℃, a reaction time of 140min and a FA/DAF lignin mass ratio of 2. The BO was recovered using ethyl acetate-water-based LLE under different pH values.

Fig. 7.1 and Fig. 7.2 present the effect of reaction solvent on BO yield and PM yield respectively. Considerably higher yields of BO and PM were obtained when MW-assisted lignin depolymerization was carried out in the ethanolic solvent system, as opposed to the aqueous solvent system. In the alkaline lignin depolymerization, BO yield for the ethanolic solvent system was 21.47% while only 6.01% for the aqueous solvent system. The difference was larger in de-alkaline lignin depolymerization, with the BO yield of 25.07% for the ethanolic solvent system and 6.67% for the aqueous solvent system. These observations are in accordance with the result reported by Oregui-Bengoechea et al. (2018) that the ethanol system yields a significantly larger

amount of BO in comparison to the water system. Oregui-Bengoechea et al. (2017) also found that ethanol served as a capping agent to stabilize highly reactive phenolic intermediates by the O-alkylation of phenolic hydroxyl groups and by the C-alkylation of aromatic rings, resulting in higher yields of BO. In terms of alkaline lignin PM yield, ethanolic solvent system contributed to a maximum PM yield of 4.35% while the yield of PM derived from aqueous solvent system was only 2.78%. Similar trend was observed in de-alkaline lignin PM yield that the transition of reaction solvent from ethanol to water resulted in a considerable decrease of PM from 4.20% to 3.10%.

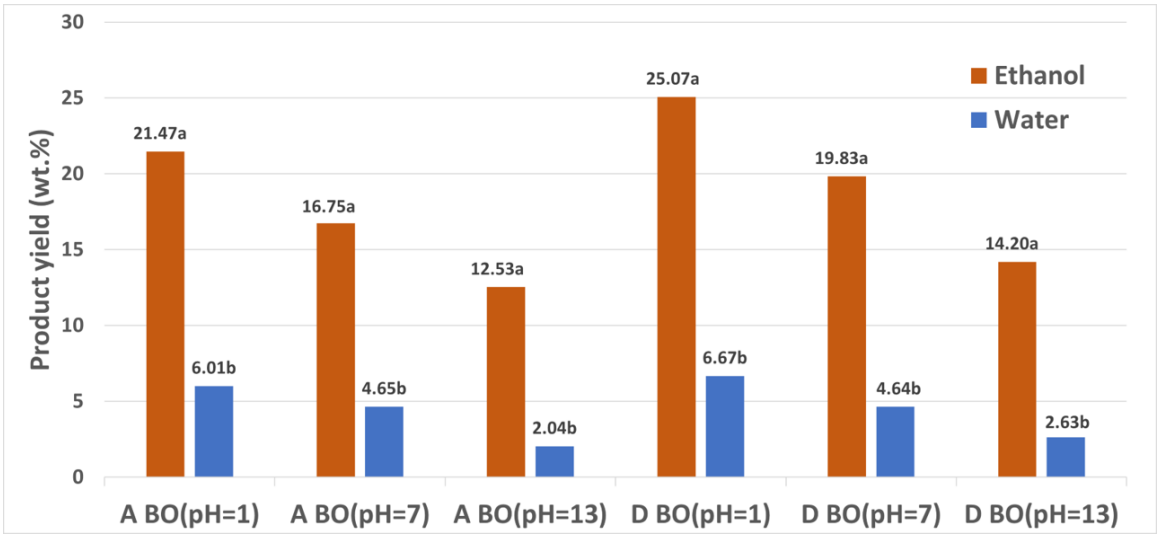

Figure 7.1 Effect of reaction solvent on BO yield
(A BO=alkaline lignin BO; D BO=de-alkaline lignin BO)

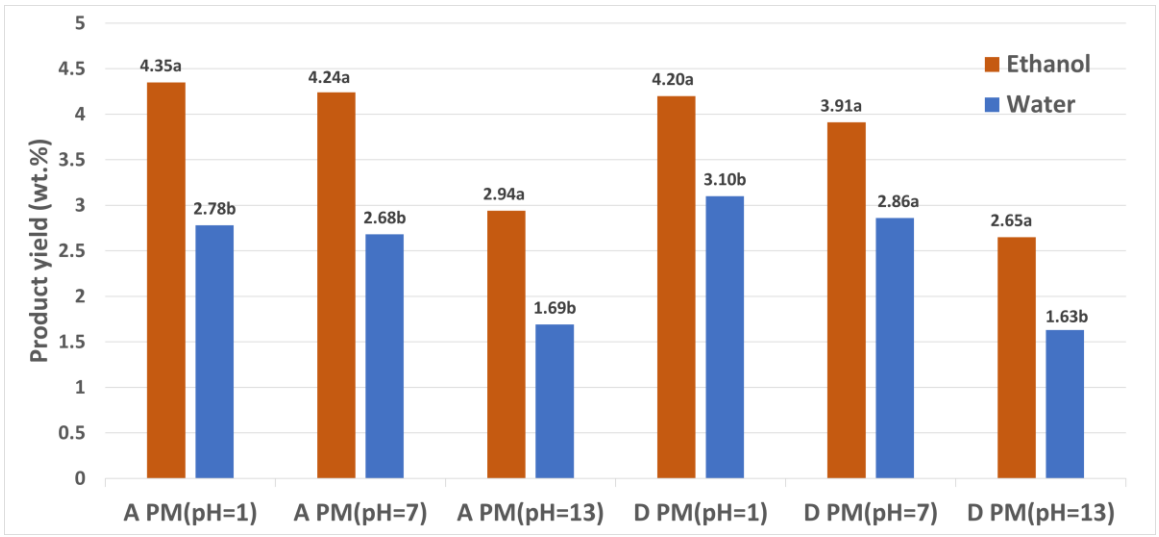

Figure 7.2 Effect of reaction solvent on PM yield
(A PM=alkaline lignin PM; D PM=de-alkaline lignin PM)

The yields of BO, SR and lignin recovery were summarized in Table 7.1. The lignin recovery yield refers to the weight percentage of lignin feedstock that could be recovered in the form of BO and SR. It is an indirect measurement of the amount of lignin that was converted into gaseous phase and the amount of lignin that was lost during the downstream procedures in the form of aqueous phase (e.g. hydrophilic phenolic compounds dissolved in aqueous phase). The lignin recovery yields are approximately 90% for ethanolic solvent system while only around 60% for aqueous solvent system. For both reaction solvent systems (e.g. ethanol or water), a higher yield of BO was usually accompanied with a lower yield of SR. Although a remarkably higher yield of BO was obtained from ethanolic solvent system as opposed to aqueous solvent system, the SR yield for ethanolic solvent system was significantly higher than that for aqueous solvent system, which is out of our expectations. This was likely due to the different natures of SR derived from two different reaction solvent systems. In ethanolic and aqueous solvent systems, SR was defined respectively as the ethanol-insoluble and water-insoluble substances with a particle size of larger than 2μm. In light of this, inorganic impurities (e.g. Na_2SO_3) in lignin feedstocks are more likely to dissolve in water than in ethanol, leading to the underestimation of SR yield derived from the aqueous solvent system.

Table 7.1 Solvent effect of ethanol and water on BO, SR and lignin recovery yields

Experiment (lignin feedstock - reaction solvent)	BO yield (wt.%)	SR yield (wt.%)	Lignin recovery yield (wt.%)
Alkaline lignin-Ethanol	17.92	74.58	92.90
De-alkaline lignin-Ethanol	21.15	66.44	87.59
Alkaline lignin-Water	5.02	57.26	62.28
De-alkaline lignin-Water	5.62	53.49	59.11

Notes: The yields of BO, SR and lignin recovery are relative to dried lignin input, not dry ash free basis

7.2. Effect of pH Level on Extraction Yields of Lignin-derived Products

In aqueous solvent system, the effect of downstream pH adjustment on product yields was also significant. From Fig. 7.3, it can be noted that the yields of BO and PM in aqueous solvent system was closely associated with the downstream pH adjustment. As the pH level decreased from 13 to 1, the yield of BO derived from alkaline lignin remarkably increased from 2.04% to 6.01%. Similar trend was observed for the yield of BO derived from de-alkaline lignin. With the increase in acidity of extraction environment, the yield of de-alkaline lignin BO gradually rose from 2.63% to 6.67%. When it comes to the PM yield, a decline in pH contributed to a remarkable

increase in alkaline lignin PM yield from 1.69% to 2.78%. The yield of de-alkaline lignin PM yield also exhibited a rising trend, from 1.63% to 3.10%.

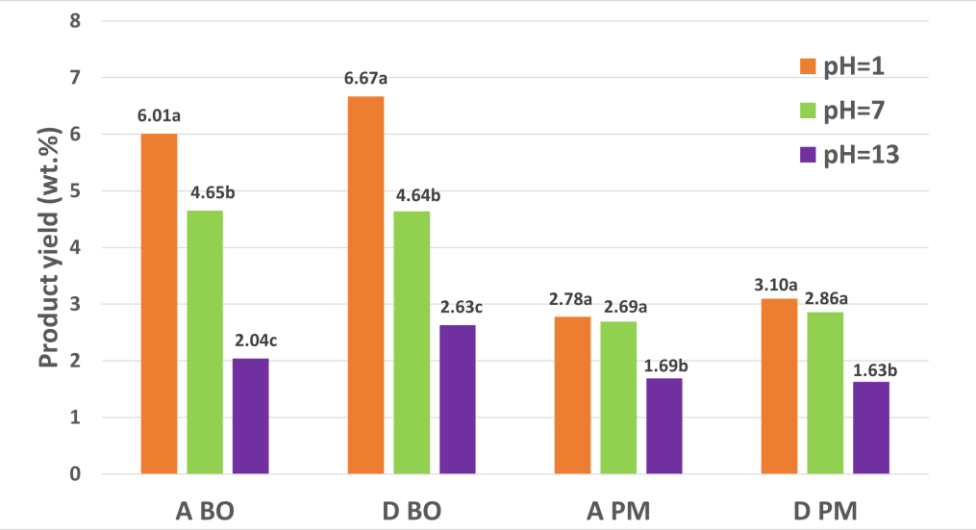

Figure 7.3 Effect of downstream pH adjustment on BO and PM yield
(A BO=alkaline lignin BO yield; D BO=de-alkaline lignin BO yield; A PM=alkaline lignin PM yield; D PM=de-alkaline lignin PM yield)

7.3. Performance of Lignin Feedstocks in Aqueous Solvent System

Alkaline and de-alkaline performed similarly in aqueous solvent system. As seen in Fig. 7.4, the type of lignin feedstocks did not have a significant effect on either BO yield or PM yield derived from MW-assisted depolymerization in aqueous solvent system. The is true for all pH level applied for downstream recovery.

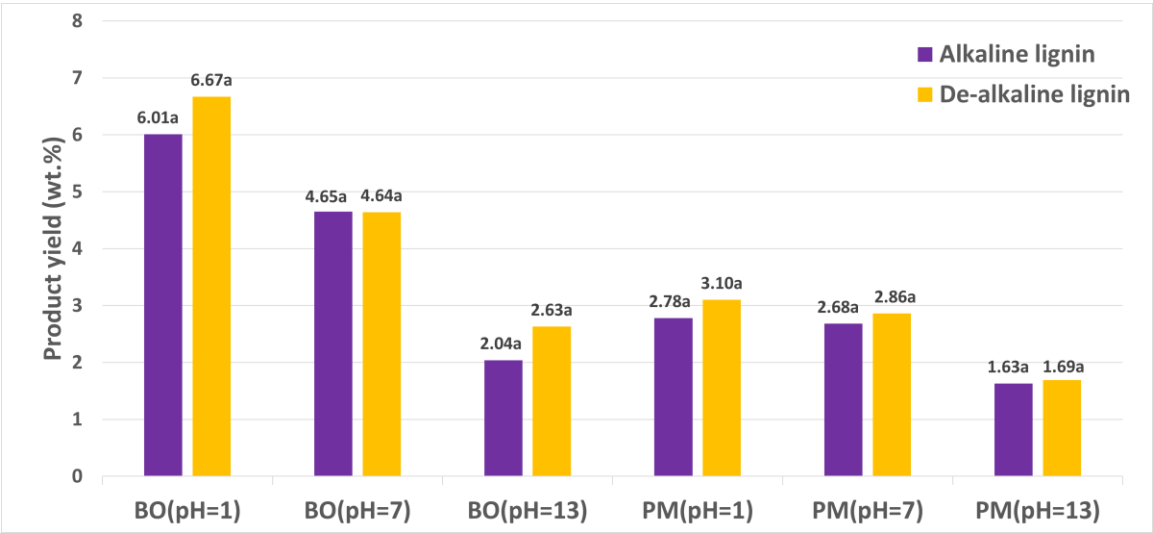

Figure 7.4 Effect of lignin feedstocks on BO and PM yields at different pH levels

7.4. GC-MS Characterization of Bio-oil from Different Solvent Systems

The GC-MS chromatograms presented in Fig 7.6 and Fig. 7.7 show the composition of GC-detectable part of the alkaline and de-alkaline lignin BO derived from ethanolic (a) and aqueous (b) solvent systems. For alkaline lignin depolymerization, the obtained BO was very similar when two different reaction solvent systems were applied (ethanol vs. water), as shown in Fig. 7.6. It is observed that guaiacol is the most abundant PM in BO derived from alkaline lignin depolymerization in either ethanolic or aqueous solvent system, under the specific reaction conditions applied in this study. However, the composition of GC-detectable part of de-alkaline lignin BO seemed to be affected by the selection of reaction solvent. Vanillin is identified as the most abundant PM in BO generated from de-alkaline lignin depolymerization in ethanolic solvent system, while aqueous solvent system resulted in guaiacol-rich BO.

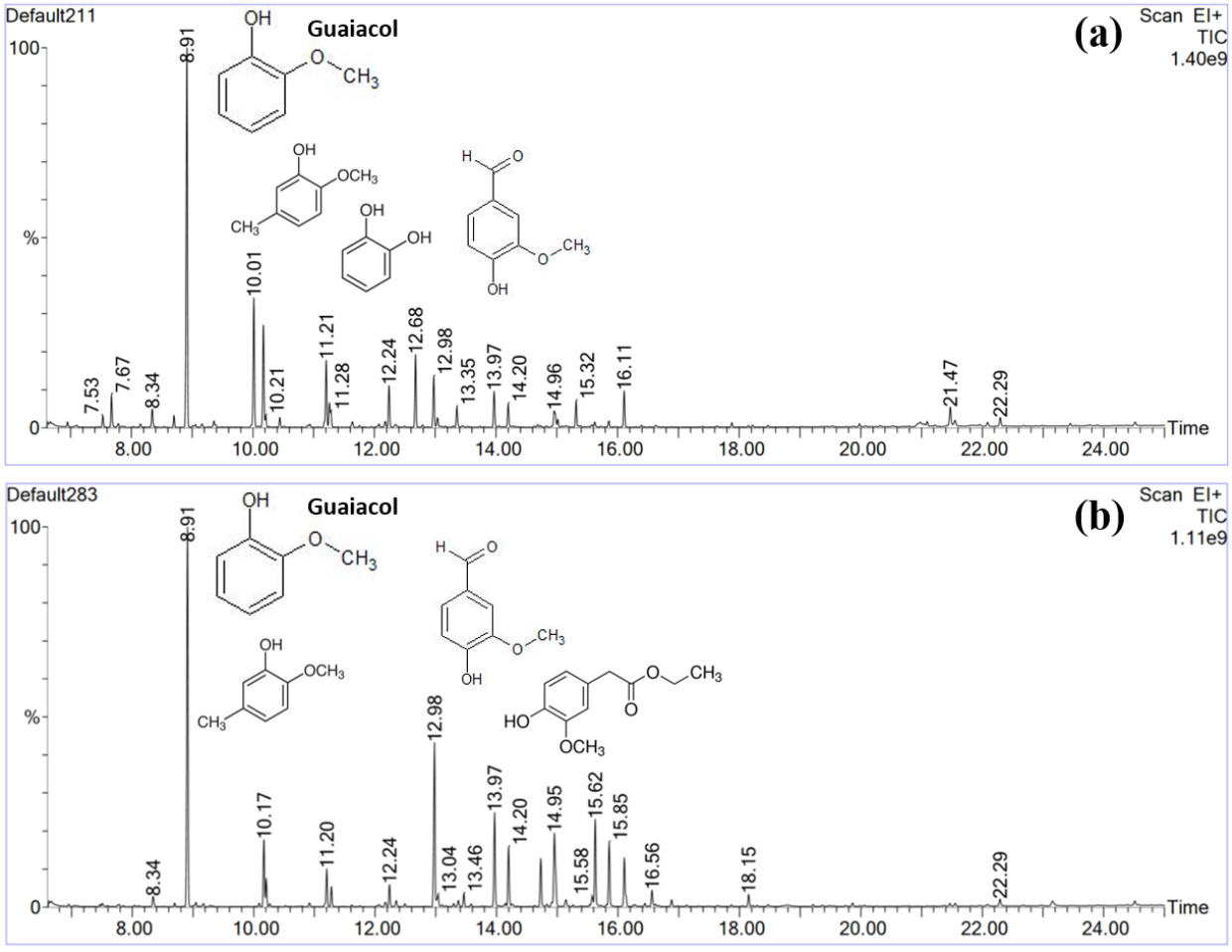

Figure 7.5 GC-MS chromatograms of alkaline lignin BO derived from ethanolic (a) and aqueous (b) solvent systems

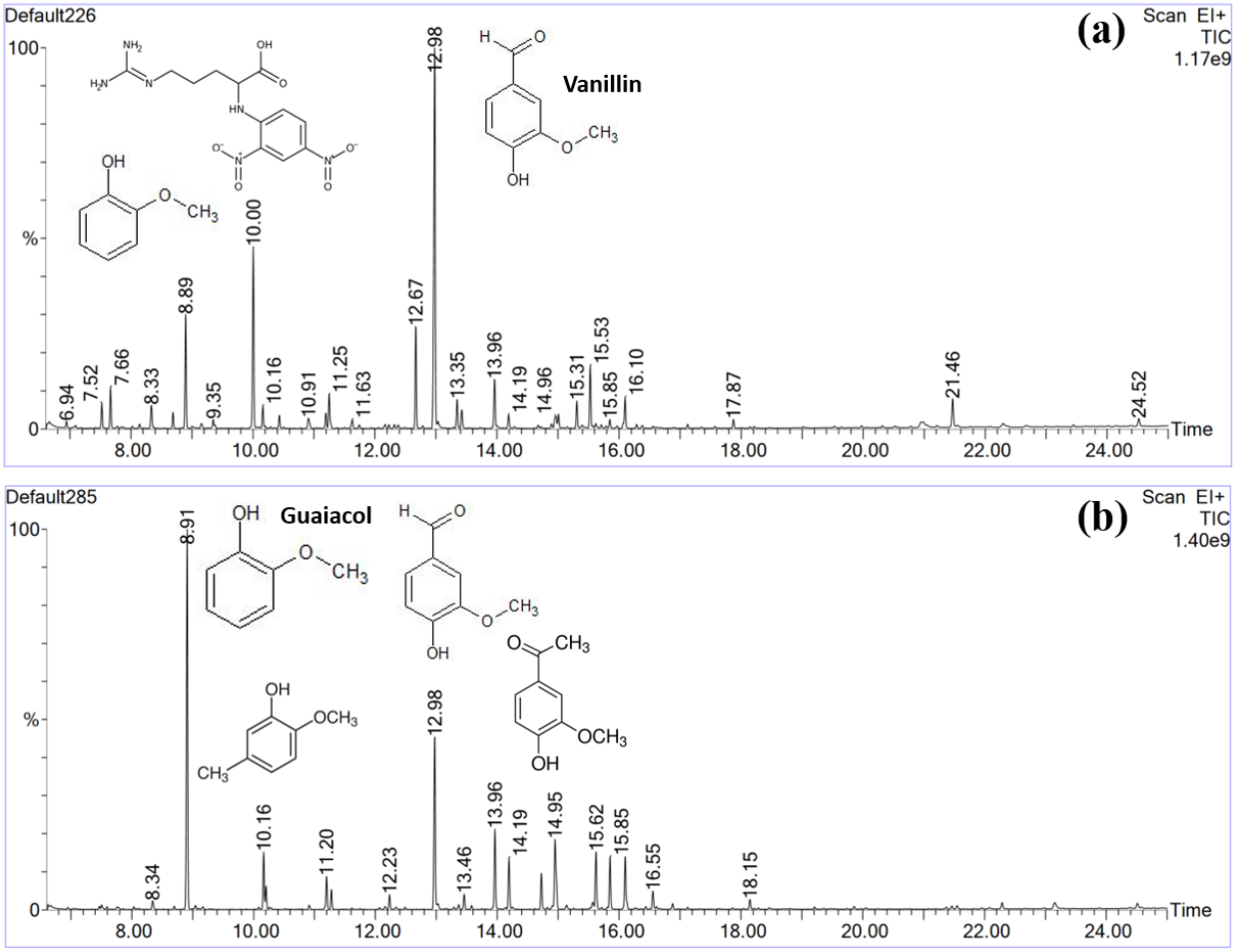

Figure 7.6 GC-MS chromatograms of de-alkaline lignin BO derived from ethanolic (a) and aqueous (b) solvent systems

7.5. Conclusions

An investigation on MW-assisted lignin depolymerization in aqueous solvent system indicated that water as a reaction medium was not effective as ethanol in lignin depolymerization in the presence of FA. The yields of BO and PM obtained from aqueous solvent system were significantly lower than those from ethanolic solvent system. The observation could be attributed to the stabilizing effect of ethanol on highly reactive phenolic intermediates generated in the process of lignin depolymerization. The extraction efficiency of lignin-derived products was closely associated with the pH adjustment prior to downstream extraction. An acidic condition was more favorable than a basic condition regarding the yields of BO and PM due to the dissociation of phenolic compounds at different pH levels. The influences of lignin feedstocks on product yields derived from MW-assisted depolymerization in aqueous solvent system were also studied. The

type of lignin feedstocks did not have a significant effect on either BO yield or PM yield, regardless of the pH level applied for downstream recovery.

Chapter 8: Overall Conclusions and Recommendations for Future Work

8.1. Overall Conclusions

MW-assisted lignin depolymerization was demonstrated to be a technically feasible and promising thermochemical technique to produce BO and PM. In our work, the effects of process variables on product yield was investigated and the reaction conditions was optimized for maximizing the yields of desired products. An efficient two-phase LLE method using both ethyl acetate and water for BO recovery was developed to improve the quality of the BO resulting from MW-assisted lignin depolymerization. In addition, the effect of reaction media including ethanol and water, on lignin depolymerization was studied. The specific conclusions corresponding to original research objectives are summarized as follows:

1. FA has the most dominant influence on the yields of BO and PM derived from MW-assisted lignin depolymerization in the ethanolic solvent system. The positive role that FA plays in lignin depolymerization also interacts with other process variables such as feedstock concentration and temperature.
2. For alkaline lignin, the optimal reactions conditions identified were feedstock concentration of 20%, FA/feedstock mass ratio of 1.5, temperature of 230℃, and retention time of 110.91min, giving the yields of BO and PM of 71.25% and 1.73% respectively. For de-alkaline lignin, the optimal reaction conditions were feedstock concentration of 17.27%, FA/feedstock mass ratio of 1.5, temperature of 208.79℃, and retention time of 140min, resulting in the yields of BO and PM of 59.40% and 2.59% respectively.
3. An “in-house” ethyl acetate-water-based downstream processing method was developed for the recovery of lignin-derived product. Extraction efficiency is pH-dependent, and the acidic condition is more favorable than the basic condition. Compared to the direct evaporation downstream processing method, the newly developed extraction method led to a remarkable decreases in BO yield while negligible changes in PM yield. However, this new method efficiently removed the impurities in the organic phase after lignin depolymerization and the quality of obtained BO was greatly improved. Two types of lignin feedstocks gave comparable BO yield and PM yield, while de-alkaline lignin BO exhibited a lower average molecular mass than alkaline lignin BO.
4. Aqueous solvent system for lignin depolymerization resulted in significantly lower yields of BO and PM than ethanolic solvent system. This might be due to the ethanol’s ability of

stabilizing highly reactive intermediates generated from depolymerization process. The depolymerization performance of the two types of lignin feedstocks presented no significant difference in aqueous solvent system, giving comparable BO and PM yields. In terms of the ethyl acetate-water-based downstream liquid-liquid extraction, the process is pH-dependent, and an acidic condition is favored to recover lignin-derived products.

8.2. Unique Contributions

Development of new biomass conversion technologies for the production of biofuel, biomaterials and value-added chemicals is mainly driven by the rapid depletion of non-renewable resources, the increasing demand for petroleum-based commodities and the negative impact on the environment due to extensive use of fossil fuels. It is essential to find and develop sustainable feedstocks and biomass conversion technologies to substitute non-renewable resources. In this work, lignin depolymerization under mild conditions with the assistance of MW, which is an energy efficient heating source, was demonstrated a feasible and promising approach for the production of BO and PM. The CCD of RSM instead of "one-factor-at-a-time" experimental design was applied to gain insights of the main and interaction effects of process variables for further optimization of reaction conditions. In addition, a new downstream processing protocol was developed for low-quality lignin feedstock containing significant amount of impurities to achieve efficient recovery of high-quality BO. Furthermore, a comparative study between ethanolic and aqueous solvent systems was carried out to study the solvent effects of two green solvents on the yield and physicochemical properties of lignin-derived products.

To summarize, the combination of renewable feedstock (lignin), energy-efficient heating source (MW heating), bio-based homogeneous catalyst (FA), and newly developed "in-house" downstream processing protocol (ethyl acetate-water-based LLE) provided an effective way to utilize waste stream, lignin for producing bio-phenolics. This will add additional income to paper and pulping processes, satisfy the diverse demand for aromatic chemicals, improve environmental sustainability, contribute to an enhanced operation of biorefinery industry, as well as provide significant opportunities for developing a low-carbon bio-economy.

8.3. Future Work

1. MW-assisted lignin depolymerization has been proved a promising method to convert lignin into value-added products in this study. The optimization of depolymerization conditions suggested that a higher temperature increased the yields of desired products.

However, the highest temperature used in this study was 230℃ due to the limitation of the microwave reactor in our lab. Therefore, it is highly recommended that a wider temperature range should be examined in future research.

2. In the depolymerization of lignin, the bio-oil yield derived from aqueous solvent system is significantly lower than that from ethanolic solvent system. This might be attributed to the faster decomposition rate of formic acid in water than in ethanol. Except the reducing effect of hydrogen from formic acid decomposition, formic acid might catalyze the depolymerization of lignin in other ways. The role of formic acid in lignin depolymerization deserves more research.
3. BO is commonly considered as the most valuable products from lignin depolymerization, and considerable efforts have been made over time to explore the physicochemical properties of BO (e.g. elemental composition, higher heating value, relative molecular mass, and volatile phenolic compounds). However, other by-product streams derived from lignin depolymerization such as the aqueous phase and the SR received very little investigations in the currently available literature. The leftover aqueous phase is suggested to be fully analyzed and the organic compounds in it are encouraged to be recovered and further used. The application of SR is worth future exploration.

References

Abbassian, K., Kargari, A., & Kaghazchi, T. (2014). Phenol Removal from Aqueous Solutions by a Novel Industrial Solvent. *Chemical Engineering Communications*. (world). Retrieved from http://www.tandfonline.com/doi/abs/10.1080/00986445.2013.848804

Agarwal, A., Rana, M., & Park, J.-H. (2018). Advancement in technologies for the depolymerization of lignin. *Fuel Processing Technology*, *181*, 115–132. https://doi.org/10.1016/j.fuproc.2018.09.017

Aguilar-Reynosa, A., Romaní, A., Ma. Rodríguez-Jasso, R., Aguilar, C. N., Garrote, G., & Ruiz, H. A. (2017). Microwave heating processing as alternative of pretreatment in second-generation biorefinery: An overview. *Energy Conversion and Management*, *136*, 50–65. https://doi.org/10.1016/j.enconman.2017.01.004

Asomaning, J., Haupt, S., Chae, M., & Bressler, D. C. (2018). Recent developments in microwave-assisted thermal conversion of biomass for fuels and chemicals. *Renewable and Sustainable Energy Reviews*, *92*, 642–657. https://doi.org/10.1016/j.rser.2018.04.084

Azadi, P., Inderwildi, O. R., Farnood, R., & King, D. A. (2013). Liquid fuels, hydrogen and chemicals from lignin: A critical review. *Renewable and Sustainable Energy Reviews*, *21*, 506–523. https://doi.org/10.1016/j.rser.2012.12.022

Bundhoo, Z. M. A. (2018). Microwave-assisted conversion of biomass and waste materials to biofuels. *Renewable and Sustainable Energy Reviews*, *82*, 1149–1177. https://doi.org/10.1016/j.rser.2017.09.066

Chen, X., Liu, Y., & Wu, J. (2020). Sustainable production of formic acid from biomass and carbon dioxide. *Molecular Catalysis*, *483*, 110716. https://doi.org/10.1016/j.mcat.2019.110716

Chen, Z., & Wan, C. (2017). Biological valorization strategies for converting lignin into fuels and chemicals. *Renewable and Sustainable Energy Reviews*, *73*, 610–621. https://doi.org/10.1016/j.rser.2017.01.166

Cheng, C., Shen, D., Gu, S., & Luo, K. (2018). State-of-the-art catalytic hydrogenolysis of lignin for the production of aromatic chemicals. *Catalysis Science & Technology*, *8*(24), 6275–6296. https://doi.org/10.1039/C8CY00845K

Chethan, S., & Malleshi, N. G. (2007). Finger millet polyphenols: Optimization of extraction and the effect of pH on their stability. *Food Chemistry*, *105*(2), 862–870. https://doi.org/10.1016/j.foodchem.2007.02.012

Dhar, P., & Vinu, R. (2017). Understanding lignin depolymerization to phenols via microwave-assisted solvolysis process. *Journal of Environmental Chemical Engineering*, *5*(5), 4759–4768. https://doi.org/10.1016/j.jece.2017.08.031

Dong, C., Feng, C., Liu, Q., Shen, D., & Xiao, R. (2014). Mechanism on microwave-assisted acidic solvolysis of black-liquor lignin. *Bioresource Technology*, *162*, 136–141. https://doi.org/10.1016/j.biortech.2014.03.060

Duan, D., Wang, Y., Ruan, R., Tayier, M., Dai, L., Zhao, Y., … Liu, Y. (2018). Comparative study on various alcohols solvolysis of organosolv lignin using microwave energy: Physicochemical and morphological properties. *Chemical Engineering and Processing - Process Intensification*, *126*, 38–44. https://doi.org/10.1016/j.cep.2017.10.023

Duval, A., & Lawoko, M. (2014). A review on lignin-based polymeric, micro- and nano-structured materials. *Reactive and Functional Polymers*, *85*, 78–96. https://doi.org/10.1016/j.reactfunctpolym.2014.09.017

Feofilova, E. P., & Mysyakina, I. S. (2016). Lignin: Chemical structure, biodegradation, and practical application (a review). *Applied Biochemistry and Microbiology*, *52*(6), 573–581. https://doi.org/10.1134/S0003683816060053

Friedman, M., & Jürgens, H. S. (2000). Effect of pH on the Stability of Plant Phenolic Compounds. *Journal of Agricultural and Food Chemistry*, *48*(6), 2101–2110. https://doi.org/10.1021/jf990489j

Ghoreishi, S., Barth, T., & Derribsa, H. (2019a). Formic acid assisted liquefaction of lignin in water and ethanol, investigated for a 0.025 and a 5 L batch reactor: Comparison of yields and compositions of the products. *Biomass and Bioenergy*, *124*, 1–12. https://doi.org/10.1016/j.biombioe.2019.03.004

Ghoreishi, S., Barth, T., & Derribsa, H. (2019b). Stirred and non-stirred lignin solvolysis with formic acid in aqueous and ethanolic solvent systems at different levels of loading in a 5-L reactor. *Biofuel Research Journal*, *6*(1), 937–946. https://doi.org/10.18331/BRJ2019.6.1.5

Hanrahan, G., & Lu, K. (2006). Application of Factorial and Response Surface Methodology in Modern Experimental Design and Optimization. *Critical Reviews in Analytical Chemistry*, *36*(3–4), 141–151. https://doi.org/10.1080/10408340600969478

Hidajat, M. J., Riaz, A., & Kim, J. (2018). A two-step approach for producing oxygen-free aromatics from lignin using formic acid as a hydrogen source. *Chemical Engineering Journal*, *348*, 799–810. https://doi.org/10.1016/j.cej.2018.05.036

Holladay, J. E., White, J. F., Bozell, J. J., & Johnson, D. (2007). *Top Value-Added Chemicals from Biomass—Volume II—Results of Screening for Potential Candidates from Biorefinery Lignin* (No. PNNL-16983, 921839; p. PNNL-16983, 921839). https://doi.org/10.2172/921839

Hu, J., Zhang, S., Xiao, R., Jiang, X., Wang, Y., Sun, Y., & Lu, P. (2019). Catalytic transfer hydrogenolysis of lignin into monophenols over platinum-rhenium supported on titanium dioxide using isopropanol as in situ hydrogen source. *Bioresource Technology*, *279*, 228–233. https://doi.org/10.1016/j.biortech.2019.01.132

Huang, S., Mahmood, N., Tymchyshyn, M., Yuan, Z., & Xu, C. (Charles). (2014). Reductive de-polymerization of kraft lignin for chemicals and fuels using formic acid as an in-situ hydrogen source. *Bioresource Technology*, *171*, 95–102. https://doi.org/10.1016/j.biortech.2014.08.045

Huang, S., Mahmood, N., Zhang, Y., Tymchyshyn, M., Yuan, Z., & Xu, C. (Charles). (2017). Reductive de-polymerization of kraft lignin with formic acid at low temperatures using inexpensive supported Ni-based catalysts. *Fuel*, *209*, 579–586. https://doi.org/10.1016/j.fuel.2017.08.031

Huang, Y., Duan, Y., Qiu, S., Wang, M., Ju, C., Cao, H., … Tan, T. (2017). Lignin-first biorefinery: A reusable catalyst for lignin depolymerization and application of lignin oil to jet fuel aromatics and polyurethane feedstock. *Sustainable Energy & Fuels*, *2*. https://doi.org/10.1039/C7SE00535K

Huang, Y.-F., Chiueh, P.-T., & Lo, S.-L. (2016). A review on microwave pyrolysis of lignocellulosic biomass. *Sustainable Environment Research*, *26*(3), 103–109. https://doi.org/10.1016/j.serj.2016.04.012

Kim, J., Lee, Y., & Kim, T. H. (2016). A review on alkaline pretreatment technology for bioconversion of lignocellulosic biomass. *Bioresource Technology*, *199*, 42–48. https://doi.org/10.1016/j.biortech.2015.08.085

Kleinert, M., Gasson, J. R., & Barth, T. (2009). Optimizing solvolysis conditions for integrated depolymerisation and hydrodeoxygenation of lignin to produce liquid biofuel. *Journal of Analytical and Applied Pyrolysis*, *85*(1–2), 108–117. https://doi.org/10.1016/j.jaap.2008.09.019

Kloekhorst, A., Shen, Y., Yie, Y., Fang, M., & Heeres, H. J. (2015). Catalytic hydrodeoxygenation and hydrocracking of Alcell® lignin in alcohol/formic acid mixtures using a Ru/C catalyst. *Biomass and Bioenergy*, *80*, 147–161. https://doi.org/10.1016/j.biombioe.2015.04.039

Kristianto, I., Limarta, S. O., Lee, H., Ha, J.-M., Suh, D. J., & Jae, J. (2017). Effective depolymerization of concentrated acid hydrolysis lignin using a carbon-supported ruthenium catalyst in ethanol/formic acid media. *Bioresource Technology*, *234*, 424–431. https://doi.org/10.1016/j.biortech.2017.03.070

Kumar, G., Shobana, S., Chen, W., Bach, Q., Kim, S., Atabani, A. E., & Chang, J.-S. (2017). A review of thermochemical conversion of microalgal biomass for biofuels: Chemistry and processes. *Green Chemistry*, *19*(1), 44–67. https://doi.org/10.1039/C6GC01937D

Lancefield, C. S., Panovic, I., Deuss, P. J., Barta, K., & Westwood, N. J. (2017). Pre-treatment of lignocellulosic feedstocks using biorenewable alcohols: Towards complete biomass valorisation. *Green Chemistry*, *19*(1), 202–214. https://doi.org/10.1039/C6GC02739C

Laurichesse, S., & Avérous, L. (2014). Chemical modification of lignins: Towards biobased polymers. *Progress in Polymer Science*, *39*(7), 1266–1290. https://doi.org/10.1016/j.progpolymsci.2013.11.004

Li, J., Dai, J., Liu, G., Zhang, H., Gao, Z., Fu, J., … Huang, Y. (2016). Biochar from microwave pyrolysis of biomass: A review. *Biomass and Bioenergy*, *94*, 228–244. https://doi.org/10.1016/j.biombioe.2016.09.010

Li, T., & Takkellapati, S. (2018). The current and emerging sources of technical lignins and their applications. *Biofuels, Bioproducts and Biorefining*, *12*(5), 756–787. https://doi.org/10.1002/bbb.1913

Liu, Q., Li, P., Liu, N., & Shen, D. (2017). Lignin depolymerization to aromatic monomers and oligomers in isopropanol assisted by microwave heating. *Polymer Degradation and Stability*, *135*, 54–60. https://doi.org/10.1016/j.polymdegradstab.2016.11.016

Liu, W., Jiang, H., & Yu, H. (2015). Thermochemical conversion of lignin to functional materials: A review and future directions. *Green Chemistry*, *17*(11), 4888–4907. https://doi.org/10.1039/C5GC01054C

Ludwig, J. R., & Schindler, C. S. (2017). Catalyst: Sustainable Catalysis. *Chem*, *2*(3), 313–316. https://doi.org/10.1016/j.chempr.2017.02.014

Milovanović, J., Rajić, N., Romero, A. A., Li, H., Shih, K., Tschentscher, R., & Luque, R. (2016). Insights into the Microwave-Assisted Mild Deconstruction of Lignin Feedstocks Using NiO-Containing ZSM-5 Zeolites. *ACS Sustainable Chemistry & Engineering*, *4*(8), 4305–4313. https://doi.org/10.1021/acssuschemeng.6b00825

Miura, M., Kaga, H., Sakurai, A., Kakuchi, T., & Takahashi, K. (2004). Rapid pyrolysis of wood block by microwave heating. *Journal of Analytical and Applied Pyrolysis*, *71*(1), 187–199. https://doi.org/10.1016/S0165-2370(03)00087-1

Montgomery, D. C. (2017). *Design and analysis of experiments* (Ninth edition..). Hoboken, NJ: John Wiley & Sons, Inc.

Motasemi, F., & Afzal, M. T. (2013). A review on the microwave-assisted pyrolysis technique. *Renewable and Sustainable Energy Reviews*, *28*, 317–330. https://doi.org/10.1016/j.rser.2013.08.008

Onwudili, J. A. (2015). Influence of reaction conditions on the composition of liquid products from two-stage catalytic hydrothermal processing of lignin. *Bioresource Technology*, *187*, 60–69. https://doi.org/10.1016/j.biortech.2015.03.088

Oregui Bengoechea, M., Hertzberg, A., Miletić, N., Arias, P. L., & Barth, T. (2015). Simultaneous catalytic de-polymerization and hydrodeoxygenation of lignin in water/formic acid media with Rh/Al2O3, Ru/Al2O3 and Pd/Al2O3 as bifunctional catalysts. *Journal of Analytical and Applied Pyrolysis*, *113*, 713–722. https://doi.org/10.1016/j.jaap.2015.04.020

Oregui-Bengoechea, M., Gandarias, I., Arias, P. L., & Barth, T. (2017). Unraveling the Role of Formic Acid and the Type of Solvent in the Catalytic Conversion of Lignin: A Holistic Approach. *ChemSusChem*, *10*(4), 754–766. https://doi.org/10.1002/cssc.201601410

Oregui-Bengoechea, M., Gandarias, I., Arias, P. L., & Barth, T. (2018). Solvent and catalyst effect in the formic acid aided lignin-to-liquids. *Bioresource Technology*, *270*, 529–536. https://doi.org/10.1016/j.biortech.2018.09.062

Ouyang, X., Huang, X., Zhu, Y., & Qiu, X. (2015). Ethanol-Enhanced Liquefaction of Lignin with Formic Acid as an in Situ Hydrogen Donor. *Energy & Fuels*, *29*(9), 5835–5840. https://doi.org/10.1021/acs.energyfuels.5b01127

Ouyang, X., Zhu, G., Huang, X., & Qiu, X. (2015). Microwave assisted liquefaction of wheat straw alkali lignin for the production of monophenolic compounds. *Journal of Energy Chemistry*, *24*(1), 72–76. https://doi.org/10.1016/S2095-4956(15)60286-8

Pandey, M. P., & Kim, C. S. (2011). Lignin Depolymerization and Conversion: A Review of Thermochemical Methods. *Chemical Engineering & Technology*, *34*(1), 29–41. https://doi.org/10.1002/ceat.201000270

Park, J., Riaz, A., Insyani, R., & Kim, J. (2018). Understanding the relationship between the structure and depolymerization behavior of lignin. *Fuel*, *217*, 202–210. https://doi.org/10.1016/j.fuel.2017.12.079

Park, S., Hong, C., Jeong, H., Lee, S., Choi, J. W., & Choi, I. (2016). Improvement of lignin oil properties by combination of organic solvents and formic acid during supercritical depolymerization. *Journal of Analytical and Applied Pyrolysis*, *121*, 113–120. https://doi.org/10.1016/j.jaap.2016.07.011

Pilar Vinardell, M., & Mitjans, M. (2017). Lignins and Their Derivatives with Beneficial Effects on Human Health. *International Journal of Molecular Sciences*, *18*(6), 1219. https://doi.org/10.3390/ijms18061219

Riaz, A., Kim, C. S., Kim, Y., & Kim, J. (2016). High-yield and high-calorific bio-oil production from concentrated sulfuric acid hydrolysis lignin in supercritical ethanol. *Fuel*, *172*, 238–247. https://doi.org/10.1016/j.fuel.2015.12.051

Schutyser, W., Renders, T., Bosch, S. V. den, Koelewijn, S., Beckham, G. T., & Sels, B. F. (2018). Chemicals from lignin: An interplay of lignocellulose fractionation, depolymerisation, and upgrading. *Chemical Society Reviews*, *47*(3), 852–908. https://doi.org/10.1039/C7CS00566K

Shao, L., Zhang, Q., You, T., Zhang, X., & Xu, F. (2018). Microwave-assisted efficient depolymerization of alkaline lignin in methanol/formic acid media. *Bioresource Technology*, *264*, 238–243. https://doi.org/10.1016/j.biortech.2018.05.083

Shen, D., Liu, N., Dong, C., Xiao, R., & Gu, S. (2015). Catalytic solvolysis of lignin with the modified HUSYs in formic acid assisted by microwave heating. *Chemical Engineering Journal*, *270*, 641–647. https://doi.org/10.1016/j.cej.2015.02.003

Strassberger, Z., Tanase, S., & Rothenberg, G. (2014). The pros and cons of lignin valorisation in an integrated biorefinery. *RSC Advances*, *4*(48), 25310–25318. https://doi.org/10.1039/C4RA04747H

Tayier, M., Duan, D., Zhao, Y., Ruan, R., Wang, Y., & Liu, Y. (2018). Catalytic Effects of Various Acids on Microwave-assisted Depolymerization of Organosolv Lignin. *BioResources*, *13*(1), 412–424.

Tayier, M., Zhao, Y., Duan, D., Zou, R., Wang, Y., Ruan, R., & Liu, Y. (2020). Bamboo biochar-catalytic degradation of lignin under microwave heating. *Journal of Wood Chemistry and Technology*, *0*(0), 1–10. https://doi.org/10.1080/02773813.2020.1741643

Toledano, A., Serrano, L., Balu, A. M., Luque, R., Pineda, A., & Labidi, J. (2013). Fractionation of Organosolv Lignin from Olive Tree Clippings and its Valorization to Simple Phenolic Compounds. *ChemSusChem*, *6*(3), 529–536. https://doi.org/10.1002/cssc.201200755

Toledano, A., Serrano, L., Labidi, J., Pineda, A., Balu, A. M., & Luque, R. (2013). Heterogeneously Catalysed Mild Hydrogenolytic Depolymerisation of Lignin Under Microwave Irradiation with Hydrogen-Donating Solvents. *ChemCatChem*, *5*(4), 977–985. https://doi.org/10.1002/cctc.201200616

Toledano, A., Serrano, L., Pineda, A., Romero, A. A., Luque, R., & Labidi, J. (2014). Microwave-assisted depolymerisation of organosolv lignin via mild hydrogen-free hydrogenolysis: Catalyst screening. *Applied Catalysis B: Environmental*, *145*, 43–55. https://doi.org/10.1016/j.apcatb.2012.10.015

Wang, C., Shi, L., Fan, L., Ding, Y., Zhao, S., Liu, Y., & Ma, C. (2013). Optimization of extraction and enrichment of phenolics from pomegranate (Punica granatum L.) leaves. *Industrial Crops and Products*, *42*, 587–594. https://doi.org/10.1016/j.indcrop.2012.06.031

Wang, H., Pu, Y., Ragauskas, A., & Yang, B. (2019). From lignin to valuable products–strategies, challenges, and prospects. *Bioresource Technology*, *271*, 449–461. https://doi.org/10.1016/j.biortech.2018.09.072

Wang, Q., Guan, S., & Shen, D. (2017). Experimental and Kinetic Study on Lignin Depolymerization in Water/Formic Acid System. *International Journal of Molecular Sciences; Basel*, *18*(10). http://dx.doi.org/10.3390/ijms18102082

Wang, Y., Leilei, D., Liangliang, F., Shaoqi, S., Yuhuan, L., & Roger, R. (2016). Review of microwave-assisted lignin conversion for renewable fuels and chemicals. *Journal of Analytical and Applied Pyrolysis*, *119*, 104–113. https://doi.org/10.1016/j.jaap.2016.03.011

Warner, J. C. (2012). Green chemistry: Theory and practice. *Abstracts of Papers of the American Chemical Society*, *244*.

Xu, C, & Ferdosian, F. (2017). *Conversion of Lignin into Bio-Based Chemicals and Materials*. Berlin Heidelberg: Springer-Verlag. https://doi.org/10.1007/978-3-662-54959-9

Xu, C, Arancon, R. A. D., & Luque, R. (2014). Lignin depolymerisation strategies: Towards valuable chemicals and fuels. *Chemical Society Reviews*, *43*(22), 7485–7500. https://doi.org/10.1039/C4CS00235K

Xu, W., Miller, S. J., Agrawal, P. K., & Jones, C. W. (2012). Depolymerization and Hydrodeoxygenation of Switchgrass Lignin with Formic Acid. *ChemSusChem*, *5*(4), 667–675. https://doi.org/10.1002/cssc.201100695

Yin, C. (2012). Microwave-assisted pyrolysis of biomass for liquid biofuels production. *Bioresource Technology*, *120*, 273–284. https://doi.org/10.1016/j.biortech.2012.06.016

You, T., Zhang, L, Zhou, S., & Xu, F. (2015). Structural elucidation of lignin–carbohydrate complex (LCC) preparations and lignin from Arundo donax Linn. *Industrial Crops and Products*, *71*, 65–74. https://doi.org/10.1016/j.indcrop.2015.03.070

Yuan, T., Xu, F., & Sun, R. (2013). Role of lignin in a biorefinery: Separation characterization and valorization. *Journal of Chemical Technology & Biotechnology*, *88*(3), 346–352. https://doi.org/10.1002/jctb.3996

Zakzeski, J., Bruijnincx, P. C. A., Jongerius, A. L., & Weckhuysen, B. M. (2010). The Catalytic Valorization of Lignin for the Production of Renewable Chemicals. *Chemical Reviews*, *110*(6), 3552–3599. https://doi.org/10.1021/cr900354u

Zhou, M., Sharma, B. K., Li, J., Zhao, J., Xu, J., & Jiang, J. (2019). Catalytic valorization of lignin to liquid fuels over solid acid catalyst assisted by microwave heating. *Fuel*, *239*, 239–244. https://doi.org/10.1016/j.fuel.2018.10.144

Zhou, M., Sharma, B. K., Liu, P., Xia, H., Xu, J., & Jiang, J. (2018). Microwave Assisted Depolymerization of Alkaline Lignin over Hydrotalcite-Based CuNiAl Mixed Oxides. *ACS Sustainable Chemistry & Engineering*, *6*(9), 11519–11528. https://doi.org/10.1021/acssuschemeng.8b01697

Zhu, Z., Rosendahl, L., Toor, S. S., & Chen, G. (2018). Optimizing the conditions for hydrothermal liquefaction of barley straw for bio-crude oil production using response surface methodology. *Science of The Total Environment*, *630*, 560–569. https://doi.org/10.1016/j.scitotenv.2018.02.194

Zou, R., Zhao, Y., Wang, Y., Duan, D., Fan, L., Dai, L., … Ruan, R. (2018). Microwave-assisted Depolymerization of Lignin with Metal Chloride in a Hydrochloric Acid and Formic Acid System. *BioResources*, *13*(2), 3704–3719.

Appendices

1. GC-MS Results of Alkaline Lignin BO

Table S.1 Major phenolic monomers in alkaline lignin BO identified by GC-MS

Peak	RT (min)	Type	Name of compound	Peak area percentage (%)
1	6.854	G	Phenol, 2-methoxy-	21.35
2	8.405	H	Creosol	23.70
3	9.640	G	Phenol, 4-ethyl-2-methoxy-	5.05
4	10.131	H	Phenol, 3-methyl-5-(1-methylethyl)-	1.66
5	10.836	G	Phenol, 2-methoxy-4-propyl-	6.48
6	11.271	G	Benzaldehyde, 3-(chloroacetoxy)-4-methoxy-	8.61
7	11.366	G	Phenol, 2-methoxy-6-(1-propenyl)-	1.28
8	11.901	G	trans-Isoeugenol	2.70
9	12.376	G	Ethanone, 1-(3-hydroxy-4-methoxyphenyl)-	8.21
10	12.907	G	Capsaicin	3.27
11	13.442	H	Acetylsalicylic acid	1.21
12	13.532	G	Benzoic acid amide, 4-hydroxy-3-methoxy-	5.76
13	14.182	G	Ethyl homovanillate	4.76
14	14.792	G	Phenylacetylformic acid, 4-hydroxy-3-methoxy-	2.62
15	20.975	G	3-(3-hydroxy-4-methoxyphenyl)-l-alanine	3.35

Note: RT=retention time, or the time from injection to detection of a certain compound, Peak area percentage=individual peak area divided by total peak area of PM and multiply the result by 100

2. GC-MS Results of De-alkaline Lignin BO

Table S.2 Major phenolic monomers in de-alkaline lignin BO identified by GC-MS

Peak	RT (min)	Type	Name of compound	Peak area percentage (%)
1	6.859	G	Phenol, 2-methoxy-	11.91
2	8.410	G	2-Methoxy-5-methylphenol	6.18
3	9.640	G	Phenol, 4-ethyl-2-methoxy-	2.49
4	10.841	G	Phenol, 2-methoxy-4-propyl-	1.97
5	11.271	G	Vanillin	32.72
6	11.376	G	trans-Isoeugenol	2.00
7	11.906	G	Phenol, 2-methoxy-4-(1-propenyl)-	2.49
8	12.376	G	Apocynin	7.11
9	12.917	G	2-Propanone, 1-(4-hydroxy-3-methoxyphenyl)-	12.01
10	13.542	G	Benzoic acid amide, 4-hydroxy-3-methoxy-	8.01
11	14.187	G	Ethyl homovanillate	3.82
12	14.297	G	Benzenepropanol, 4-hydroxy-3-methoxy-	3.69
13	14.797	G	Phenylacetylformic acid, 4-hydroxy-3-methoxy-	3.31
14	15.027	H	benzene, 1-[(2,2-diethoxyethyl)thio]-3-methyl-	2.30

Note: RT=retention time, or the time from injection to detection of a certain compound, Peak area percentage=individual peak area divided by total peak area of PM and multiply the result by 100

3. Details of Newly Developed BO Recovery Method

The detailed “in-house” downstream recovery method adapted in this study was described stepwise as follows:

1. After the reaction was completed, the product mixture was transferred from the quartz vessel to a beaker, and the inner wall of the vessel was rinsed with suitable amount of ethanol.
2. The product mixture was filtered through a 2μm filter paper, a 0.45μm syringe filter, and a 0.2μm syringe filter.
3. The pH level of the filtrate was adjusted to acidic level (pH=1), neutral level (pH=7), or basic level (pH=13) with 2M hydrochloric acid (HCl) solution or 2M sodium hydroxide (NaOH) solution. The obtained filtrates were designated as “acidic (A) filtrate”, “neutral (N) filtrate”, and “basic (B) filtrate”. (Notes: Literally pH is a measurement of the concentration of hydrogen ions in aqueous solution)
4. “A”, “N” and “B” filtrates were carefully transferred into three separatory funnels respectively, followed by the addition of 50mL of ethyl acetate for extraction. After gently shaking the funnels and venting for a few times, the observed phenomena were shown in Fig. 6.2 and Fig. 6.3. From Fig 6.2, it can be observed that beige-color flocculation appeared and gradually settled down to the bottom of “A” funnel, while small aquoues layers were noticed in “N” and “B funnels” containing filtrates from alkaline lignin. According to Fig 6.3, no flocculation was observed in “A” funnel, while small aquoues layers were noted in “N” and “B funnels” containing filtrates from de-alkaline lignin.

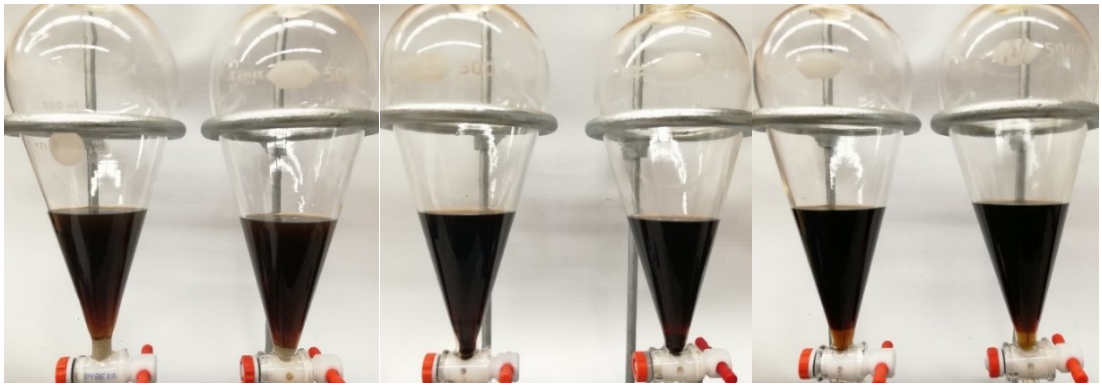

Figure S.1 Phenomena observed in funnels containing “A”, “N”, and “B” filtrates from alkaline lignin when 50ml ethyl acetate was added

Figure S.2 Phenomena observed in funnels containing "A", "N", and "B" filtrates from de-alkaline lignin when 50ml ethyl acetate was added

5. 60mL of distilled water was added into "A", "N" and "B" funnels respectively, followed by mild oscillation, placing the separatory funnels back in the iron rings and waiting for a few minutes to allow for the separation of layers, as presented in Fig. 6.4 and Fig. 6.5. Two immiscible layers were found in all separatory funnels. The upper layer was organic phase containing phenolic BO while the bottom layer was aqueous phase.

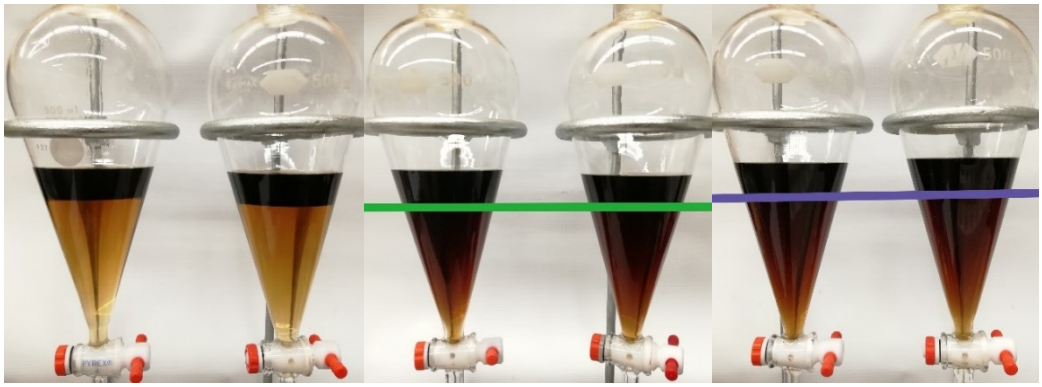

Figure S.3 Phenomena observed in funnels containing "A", "N", and "B" filtrates from alkaline lignin when 50ml ethyl acetate and 60ml water were added

Figure S.4 Phenomena observed in funnels containing "A", "N", and "B" filtrates from de-alkaline lignin when 50ml ethyl acetate and 60ml water were added

6. Repeat Step 5 and need to watch out very carefully to avoid emulsions during oscillation because a large amount of distilled water (120mL) had been added into the system. The phenomena observed were shown in Fig. 6.6 and Fig. 6.7.

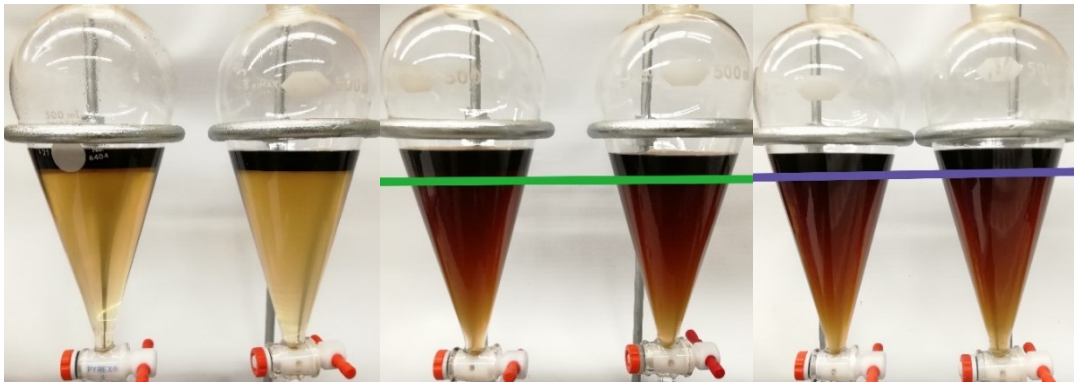

Figure S.5 Phenomena observed in funnels containing "A", "N", and "B" filtrates from alkaline lignin when 50ml ethyl acetate and 120ml water were added

Figure S.6 Phenomena observed in funnels containing "A", "N", and "B" filtrates from de-alkaline lignin when 50ml ethyl acetate and 120ml water were added

7. As the upper organic layer contains our desired product, the stopper on the top of the funnel was removed and the bottom aqueous layer was drained down into a clean container for further analysis. Fig. 6.8 shows the aqueous phase derived from LLE of alkaline and de-alkaline lignin filtrates.

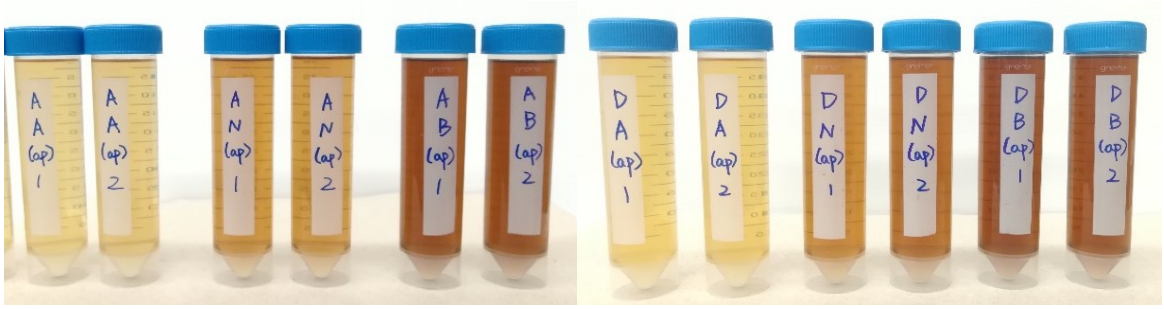

Figure S.7 Aqueous phase derived from LLE of alkaline and de-alkaline lignin filtrates

8. 60mL distilled water was added into the separatory funnel to wash the leftover organic phase without oscillation, as shown in Fig. 6.9 and Fig. 6.10. Jelly-like emulsions were observed in all separatory funnels, and an enlarged view of emulsions was presented in Fig. 6.11.

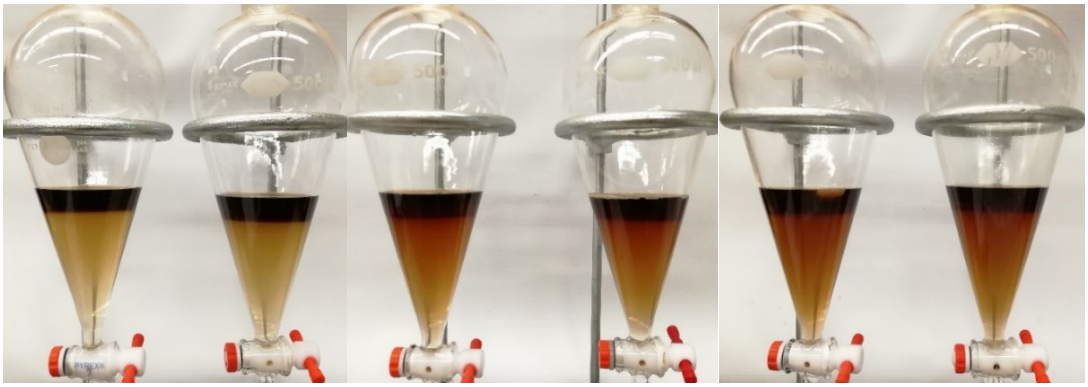

Figure S.8 Phenomena observed in funnels containing "A", "N", and "B" filtrates from alkaline lignin when additional 60ml water was added

Figure S.9 Phenomena observed in funnels containing "A", "N", and "B" filtrates from de-alkaline lignin when additional 60ml water was added

Figure S.10 the observed jelly-like emulsions when additional 60ml water was added

9. 6g of anhydrous sodium sulfate (Na_2SO_4) was added into the separatory funnel to increase the surface tension of the droplets and increase the density of aqueous layer, which further help to destroy emulsions and force separation, as presented in Fig. 6.12 and Fig. 6.13.

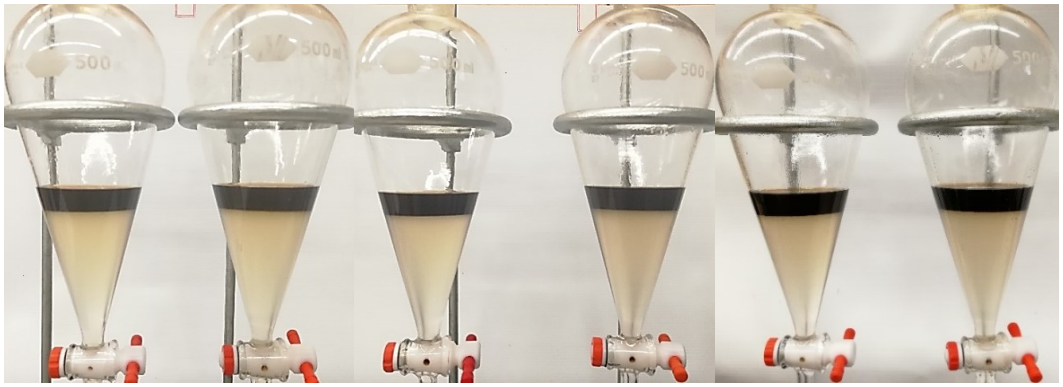

Figure S.11 Phenomena observed in funnels containing "A", "N", and "B" filtrates from alkaline lignin when emulsions were broken

Figure S.12 Phenomena observed in funnels containing "A", "N", and "B" filtrates from de-alkaline lignin when emulsions were broken

10. The bottom aqueous layer was carefully drained down and the upper organic layer was dried over 2g of anhydrous Na_2SO_4 to remove the possibly existing water. The water-free organic phase was then filtered through a 0.2μm syringe filter, followed by the rotary evaporation of organic solvent (ethyl acetate and ethanol) at reduced pressure and 70℃ to obtain BO. The alkaline lignin BO and de-alkaline lignin BO are shown in Fig 6.14 and Fig. 6.15 respectively.

Figure S.13 Alkaline lignin BO derived from "A", "N", and "B" filtrates

Figure S.14 De-alkaline lignin BO derived from "A", "N", and "B" filtrate